TALLINN UNIVERSITY OF TECHNOLOGY

FACULTY OF CHEMICAL AND MATERIALS TECHNOLOGY

DEPARTMENT OF MATERIALS SCIENCE

GRID-CONNECTED PHOTOVOLTAIC SYSTEM DESIGN FOR A SHOPPING CENTER IN TARTU

Master Thesis

Utku Dinler

Supervisor : Andres Öpik , Chair of Physical Chemistry,

Professor

Materials and Processes of Sustainable Energetics

2014

Declaration

Hereby I declare that this master thesis, my original investigation and achievement, submitted for the master degree at Tallinn University of Technology has not been submitted for any degree or examination.

.....

Name of the student

TALLINNA TEHNIKAÜLIKOOL

KEEMIA- JA MATERJALITEHNOLOOGIA TEADUSKOND

MATERJALITEADUSE INSTITUUT

TARTU KAUBANDUSKESKUSE JAOKS GENEREEERİTUD VÕREGA-ÜHENDATUD PÄİKESEPANEELİ SÜSTEEM

Magistritöö

Utku Dinler

Juhendaja : Andres Öpik , füüsikalise keemia õppetool,

Professor

Materjalid ja protsessid jätkusuutlikus energeetikas

2014

Table of Contents

Abbreviations and Acronyms

Air Mass	(AM)
Alternate Current	(AC)
Direct Current	(DC)
Incidence Angle Modifier	(IAM)
Kilowatt hour	(kWh)
Kilowatt peak	(kWp)
Light Induced Degradation	(LID)
Maximum Power Point	(MPP)
Meter	(m)
Nominal Operating Cell Temperature	(NOCT)
Photovoltaic	(PV)
Standard Test Conditions	(STC)
Solar Constant	(E_q)

1. Introduction

As demand for significantly increases all around the world, environmental effects and limited sources of fossil fuels has led the countries to invest in renewable energy technologies.

European Union aims to provide 20% of its energy from renewables by 2020 in order to cut the greenhouse gas emissions and be less dependent on imported energy [1]. As a member of European Union, Estonia, provided 14.6% of its energy supply from renewables in 2012, which is a result of using biomass in heating sector. In addition, Estonia has significant potential of wind energy [2].

Developments in photovoltaic system during the last decade have shown that it can be an economically viable option in northern countries and diversify the choices of renewable energy.

The objective of this thesis is to design sufficient grid-connected photovoltaic systems for a shopping mall in Tartu, Estonia.

The aim of this thesis is to compare the performances and investigate the economical aspects of the designed photovoltaic systems and offer the most suitable inverter type.

2. Introduction to Solar Energy

Solar energy is the energy that comes to Earth from the core of the Sun, which is created from the conversion of hydrogen to helium. It comes to Earth as electromagnetic waves (photons). Since it is available everywhere, it is free of geopoloitical tensions and free of pollution emissions.

Although many efficient systems of solar energy to produce heat and electricity had been demonstrated, it has not yet been accepted as a common source of energy because of economic competition against cheaper fossil fuels and the contuniuty and reliability issues that modern economies and lifestyles demand [3].

2.1. Solar Radiation

Solar radiation is defined as the electromagnetic radiation that is transmitted from the Sun [4]. Because of the long distance between the Sun and the Earth, only an insignificant proportion of the radiation arrives to the Earth, which attains an amount of energy 10^{18} kWh/year. This amount of energy is almost 10.000 times of the energy requirement in the world [5].

2.1.1. Distribution of Solar Radiation

The amount of solar radiation outside the atmosphere of the Earth changes as the Earth moves in the orbit of the Sun (Figure 2.1). The change in the distance results as a fluctuation in the irradiance which is between 1325 W/m^2 and 1412 W/m^2. The average value is defined as solar constant, E_q, which is 1367 W/m^2. Because of the losses of insolation in Earth's athmosphere which is caused by reflection, absorption (by ozone, water vapour, oxygen and carbon dioxide) and scattering (by air molecules, dust particles or pollution), this amount of irradiance cannot reach on the Earth's surface most of the time, but it can peak up to 1400 W/m^2 for short periods, depending on the clouds.

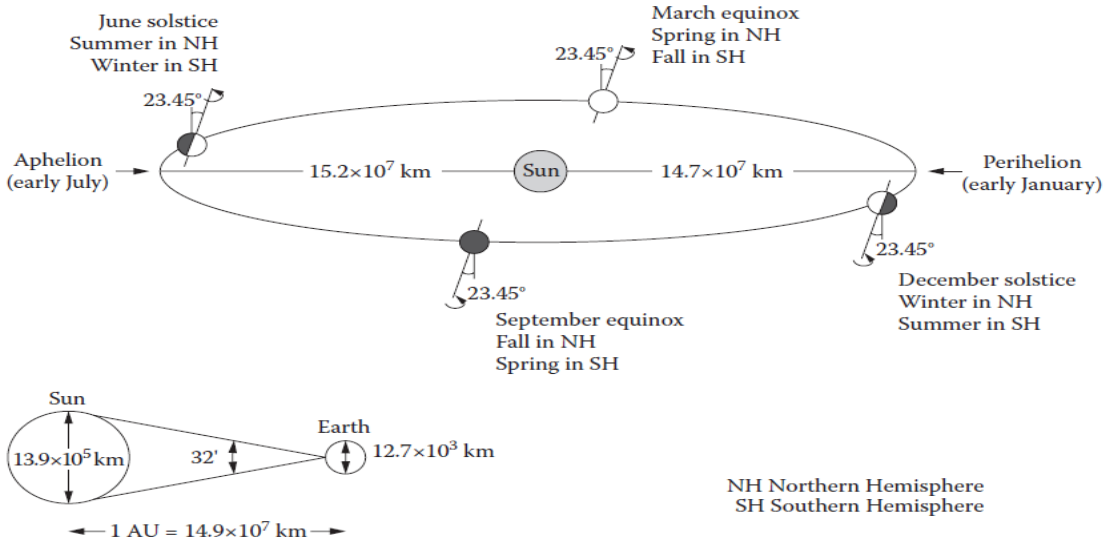

Figure 2.1 Annual motion of the Earth around the Sun [1]

The annual global radiation is defined as the total energy content of solar radiation over a year. It changes abundantly according to the region as shown in Figure 2.2.

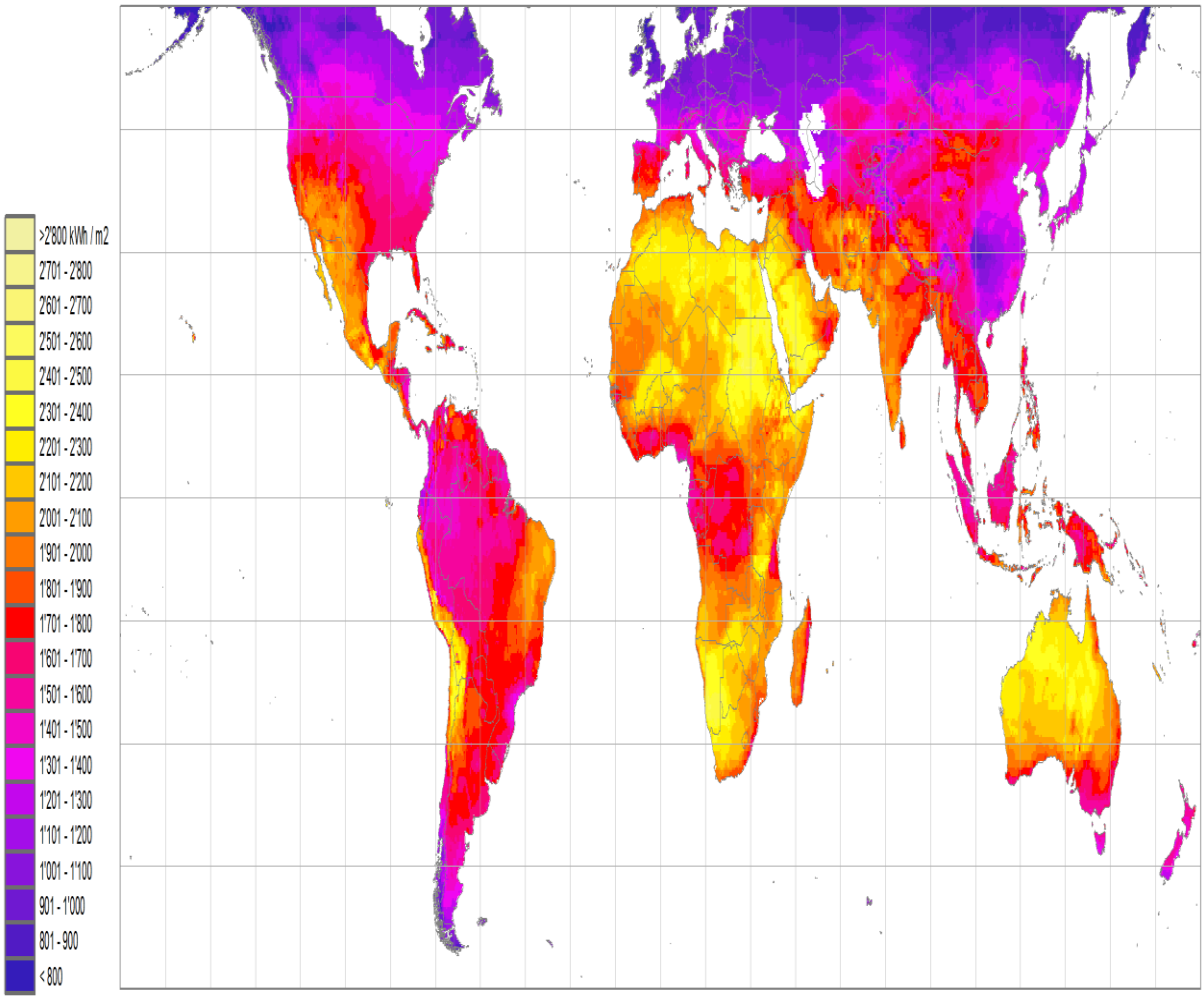

Figure 2.2 Yearly sum of global irradiance [6]

2.1.2. Direct and Diffuse Radiation

The solar radiation on the Earth's surface is a composition of direct radiation and diffuse radiation. Diffuse radiation is scattered at the sky and has no direction, unlike direct radiation which comes directly from sky and forms shadows on objects. The proportions of direct and diffuse radiation depends on cloud conditions and solar altitude [5]. Figure 2.3 shows an illustration of direct and diffuse radiation.

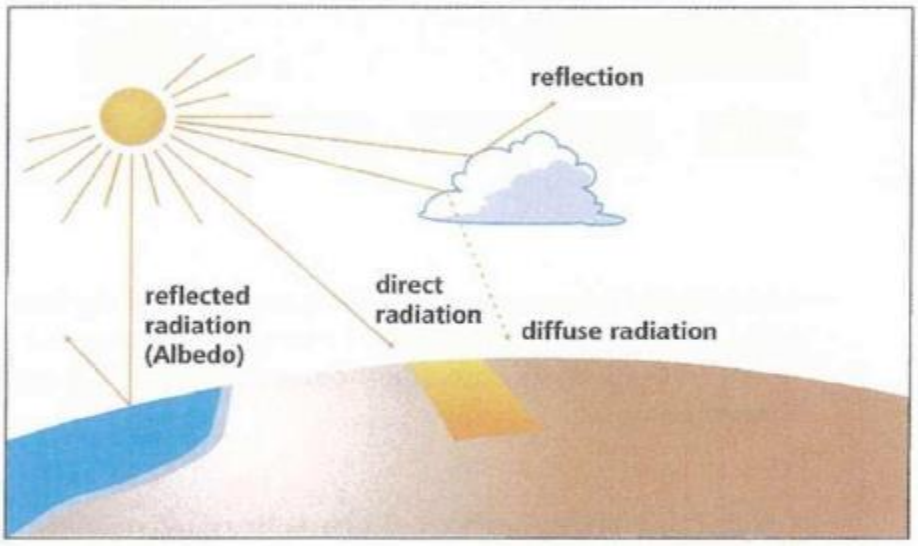

Figure 2.3 Sunlight as it passes through the atmosphere [3]

2.1.3. Air Mass

When the Sun is perpendicular to the Earth's surface, the sunlight goes through the minimum distance possible in the air mass of the atmosphere. Therefore, the maximum irradiance usually occurs on a surface which is perpendicular to the direct sunlight. Figure 2.4 shows the relationship between air mass and sunlight during the year for Berlin.

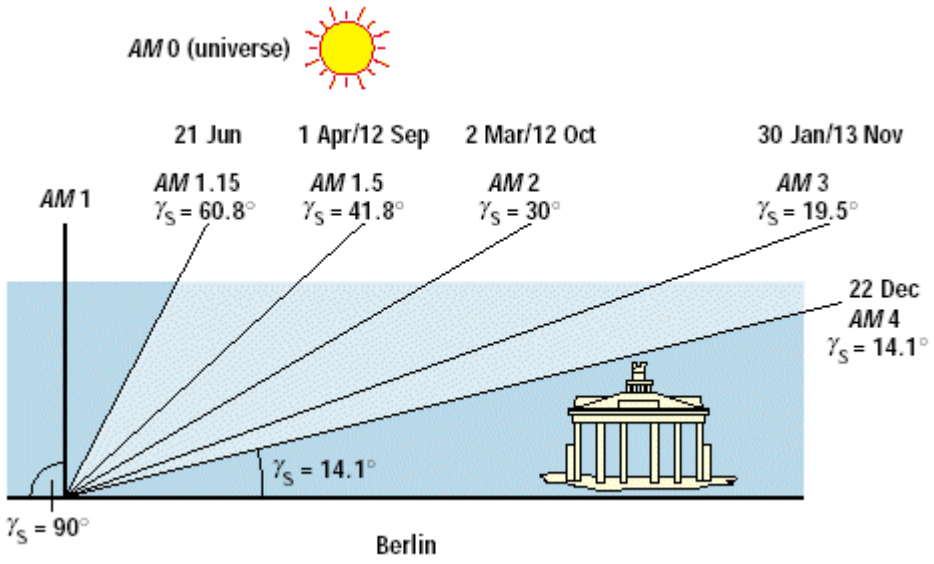

Figure 2.4 Air mass during the year in Berlin [7]

2.1.4. Sun height, Zenith Angle and Azimuth Angle

Sun height is the angle between the horizon and the center of the Sun (γ_S) and the zenith angle is defined as the opposite of the sun height, which is 90° - γ_S .

Azimuth angle (α_S) is the angle between the geographical North and the point on the horizon below the Sun and it is measured clockwise. The angles are shown in Figure 2.5.

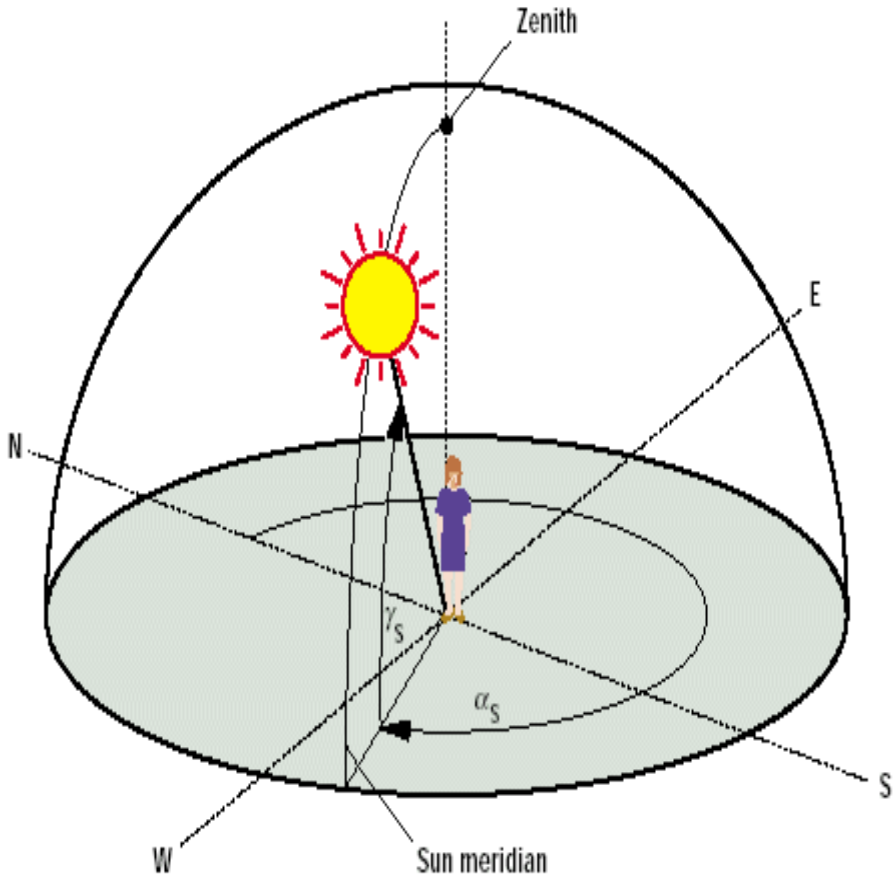

Figure 2.5 Sun height, Zenith angle and Azimuth angle [7]

2.1.5. Optimal Solar System Orientation

Figure 2.6 shows the angles of the sun, azimuth angle and tilt angle to define the orientation of a tilted surface. All these angles has to be taken into account to define an angle of incidence (θ). Figure 2.6 visualizes the sun angles, azimuth and tilt angle to define the position of a tilted surface. The angle of incidence θ depends on all these angles. The maximum irradiance can usually be obtained by a surface that is perpendicular to the sun.

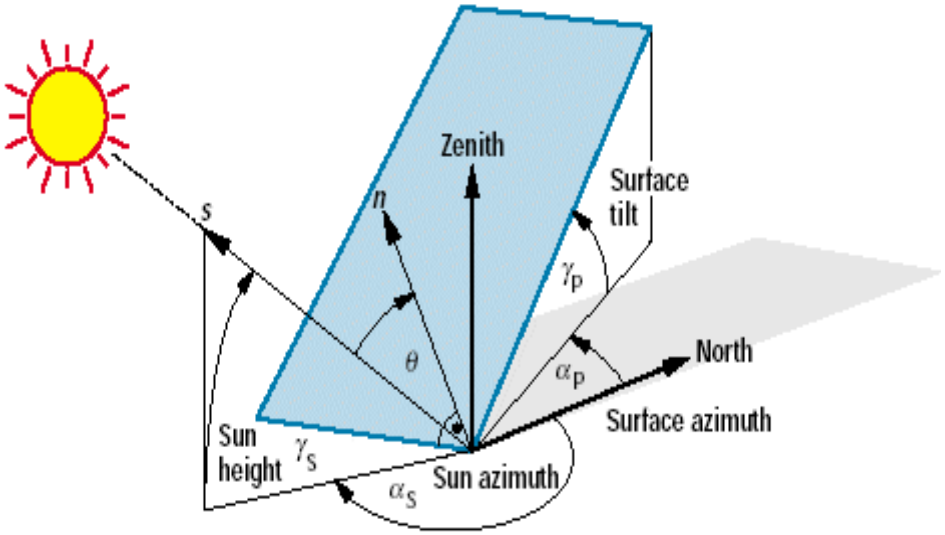

Figure 2.6 Angles to define the position of the Sun and the orientation of a tilted plane [7]

3. Photovoltaic Modules and Systems

Photovoltaic (PV) modules are devies which uses solar radiation, the most common energy source in the world, to generate electricity without a heat engine or a rotating equipment, without any moving parts. Therefore, they require minimum maintenance and can be used for a long period of time. They do not produce any pollution.

There is no size limitation for photovoltaic systems and since they are modular systems the sizes can ben increased by adding more panels to the system. They can also be used as stand-alone systems.

In the past, the energy required to produce a PV module was more than the energy it produces in its lifetime. As a result of the developments in the production of PV modules during the last decade, now the payback times are around 3-5 years, depending on the location of the installation. In 2013, the cost of photovoltaics are $2.5 US per watt peak and the goal is to reduce it to $1 US per watt peak [8]. In the forth quater of 2014, the average total installed cost of a rooftop PV cost has been $3.6 US per watt, including modules, inverters, direct labor, engineering and other system components, module prices decreasing down to $0.69 per watt for large order volumes [9].

In 2012, due to the remarkable growth in the past decade, the total PV capacity of the world was 102 GW, which can produce as much energy as 16 coal plants, saving 53 million tons of carbon [10]. In 2013, it reached to 136.7 GW as Asian market takes the lead over European

market. The global evolutions of installations and cumulative installed capacities between 2000 and 2013 are shown in Figure 3.1 and Figure 3.2.

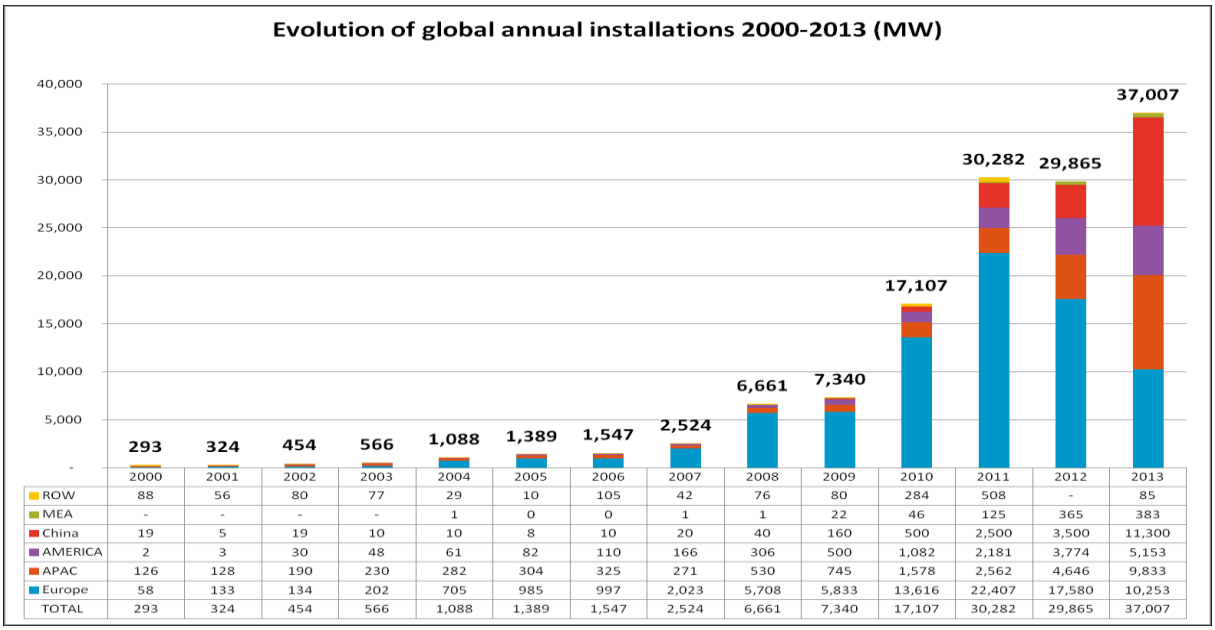

	2000	2001	2002	2003	2004	2005	2006	2007	2008	2009	2010	2011	2012	2013
ROW	88	56	80	77	29	10	105	42	76	80	284	508	-	85
MEA	-	-	-	-	1	0	0	1	1	22	46	125	365	383
China	19	5	19	10	10	8	10	20	40	160	500	2,500	3,500	11,300
AMERICA	2	3	30	48	61	82	110	166	306	500	1,082	2,181	3,774	5,153
APAC	126	128	190	230	282	304	325	271	530	745	1,578	2,562	4,646	9,833
Europe	58	133	134	202	705	985	997	2,023	5,708	5,833	13,616	22,407	17,580	10,253
TOTAL	293	324	454	566	1,088	1,389	1,547	2,524	6,661	7,340	17,107	30,282	29,865	37,007

Figure 3.1 Evolution of global annual installations [11]

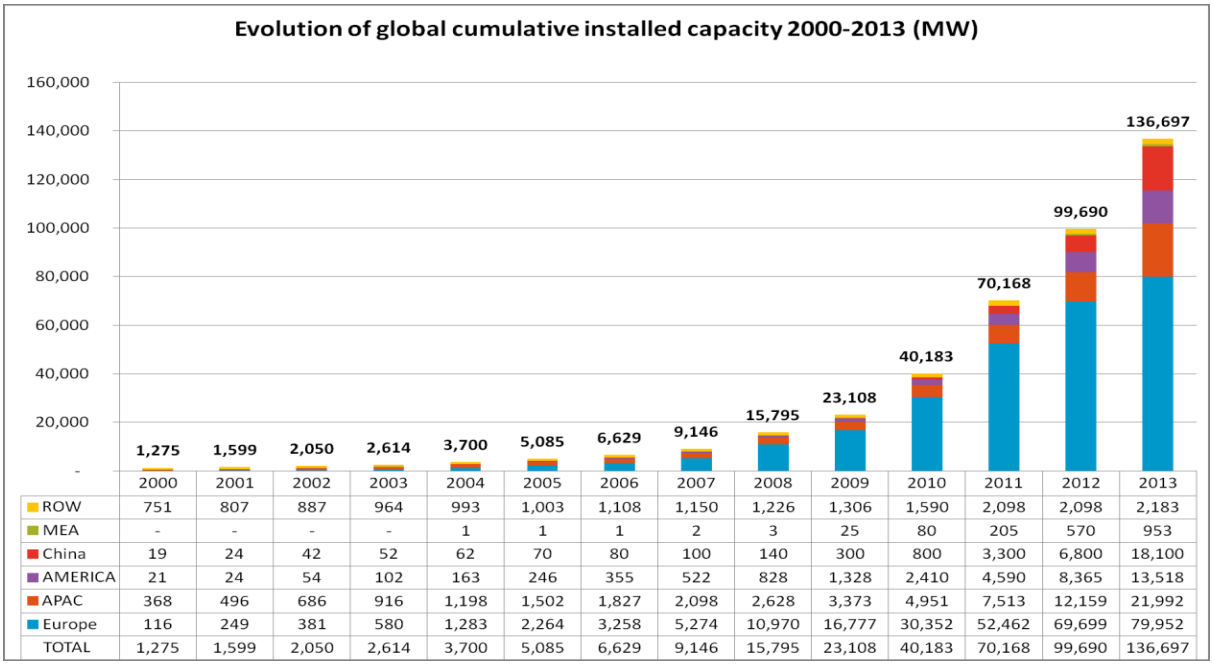

	2000	2001	2002	2003	2004	2005	2006	2007	2008	2009	2010	2011	2012	2013
ROW	751	807	887	964	993	1,003	1,108	1,150	1,226	1,306	1,590	2,098	2,098	2,183
MEA	-	-	-	-	1	1	1	2	3	25	80	205	570	953
China	19	24	42	52	62	70	80	100	140	300	800	3,300	6,800	18,100
AMERICA	21	24	54	102	163	246	355	522	828	1,328	2,410	4,590	8,365	13,518
APAC	368	496	686	916	1,198	1,502	1,827	2,098	2,628	3,373	4,951	7,513	12,159	21,992
Europe	116	249	381	580	1,283	2,264	3,258	5,274	10,970	16,777	30,352	52,462	69,699	79,952
TOTAL	1,275	1,599	2,050	2,614	3,700	5,085	6,629	9,146	15,795	23,108	40,183	70,168	99,690	136,697

Figure 3.2 Evolution of global cumulative installed capacity [11]

Although the European market of photovoltaics has declined after a long time, it is expected to stabilize or slightly decline as shown in the forecasts of PV market in Europe based on a

Business-as-Usual scenario (without any support from policymakers), and a Policy-Driven scenario until 2017, as shown in Figure 3.3.

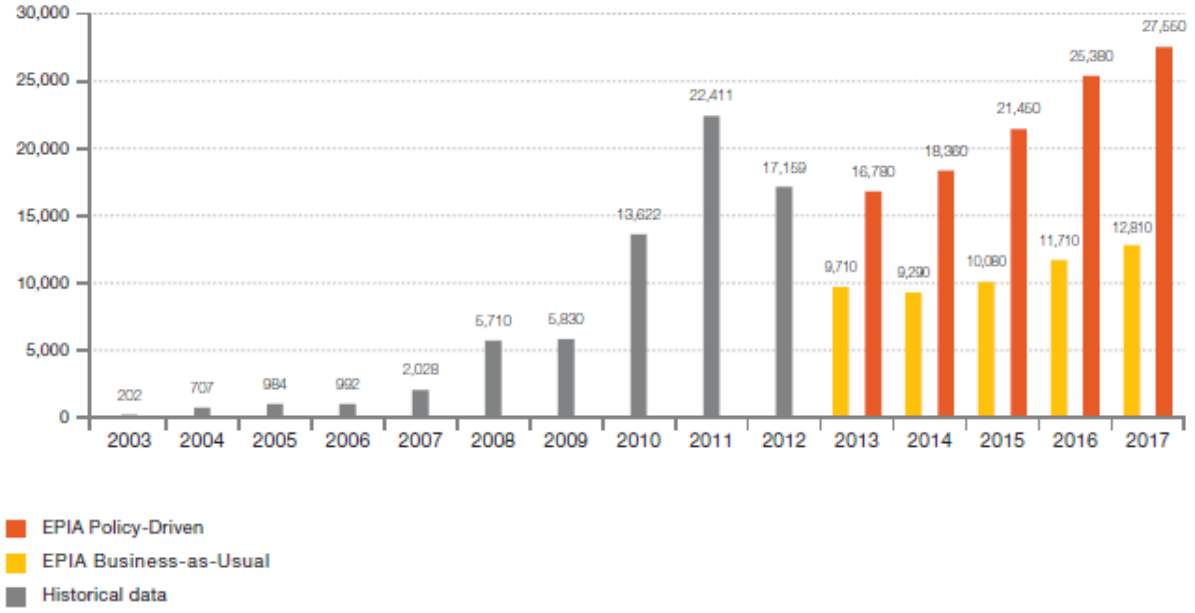

Figure 3.3 European annual PV market scenarios until 2017 (MW) [10]

According to the report of International Energy Agency, the PV market has improved with a globally limited growth, with differences between regions. Asia has become the leading region for PV installations, with the stable market of China (more than 10 GW) and rapid growth of the Japanese market (more than 9.7 GW).

The market in Europe continued to decline, regardless of the growth in the UK (first place in Europe with 2.27 GW in 2014) and France. German market did not improve in 2014 (1.9 GW) along a highly competitive approach in incentives.

177 GW total capacity of PV systems have been installed around the world as of 2014, with a fraction of 38.7 GW just in 2014. According to the latest data, only %1 of the total electricity production is covered by PV systems and 19 countries have enough PV installations to cover at least %1 of their electricty production. Figure 3.4 shows the evolution of PV installations until 2014 and Figure 3.5 shows top countries for installations and total installed capacity in 2014 [12].

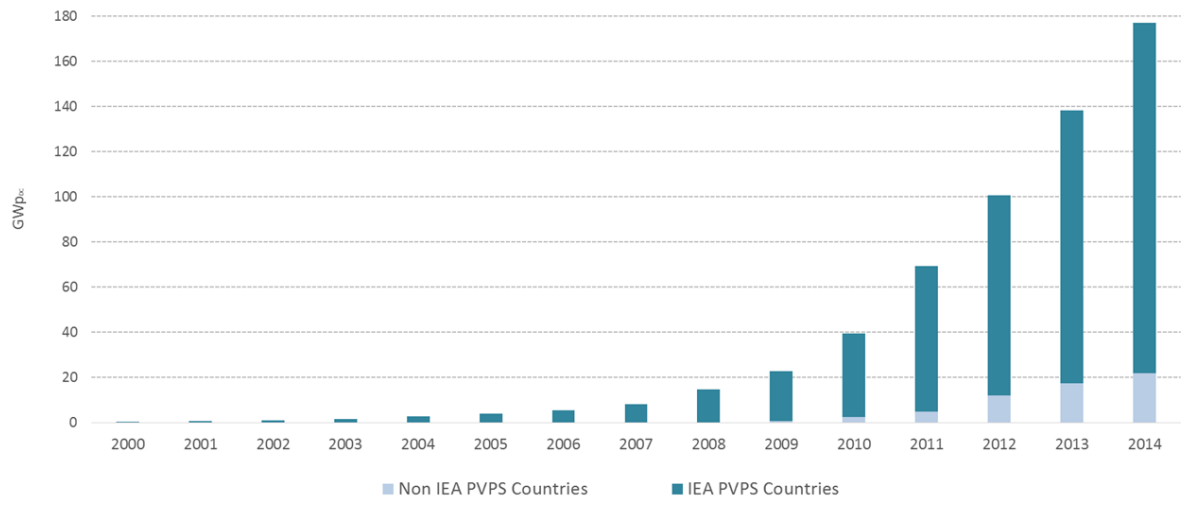

Figure 3.4 Evolution of PV installations until 2014 [12]

	TOP 10 COUNTRIES IN 2014 FOR ANNUAL INSTALLED CAPACITY		TOP 10 COUNTRIES IN 2014 FOR CUMULATIVE INSTALLED CAPACITY	
1st	China	10,6 GW	Germany	38,2 GW
2nd	Japan	9,7 GW	China	28,1 GW
3rd	USA	6,2 GW	Japan	23,3 GW
4th	UK	2,3 GW	Italy	18,5 GW
5th	Germany	1,9 GW	USA	18,3 GW
6th	France	0,9 GW	France	5,7 GW
7th	Australia	0,9 GW	Spain	5,4 GW
8th	Korea	0,9 GW	UK	5,1 GW
9th	South Africa	0,8 GW	Australia	4,1 GW
10th	India	0,6 GW	Belgium	3,1 GW

Figure 3.5 Top countries for installations and total installed capacity in 2014 [12]

3.1. Semiconductors

PV cells use two or more thin layers of semiconducting material. Silicon (Si) is the most common material that is used, along with compounds of cadmium sulphide (CdS), cuprous sulphide (Cu_2S), and gallium arsenide (GaAs). Silicon is found abundantly (one quarter of the Earth's crust is silicon). It is a cheap mineral but in order to be used it has to be processed. It is expected that developments in the production processes of silicon will lower the prices in the next years.

Recently, different types of materials such as cadmium telluride (CdTe) and copper indium diselenide (CIS) have been used in PV modules since they can be produced by relatively inexpensive industrial processes and deliver higher module efficiencies than silicon.

Exposure of light on the silicon creates an electrical charge and it can be conducted with metal conductors as direct current. PV cells are combined, usually with a glass cover to form modules (panels).

The electrons that are closer to the nucleus in an atom require a great amount of energy to become free from the attraction of the nucleus. The electronic energy of individual atoms change as the atoms get closer and the energy levels are grouped in energy bands. The electrons at the outermost shell of the atoms are the only ones that interact with other atoms, and this band is called the valence band.

Electrons in the valence band are loosely attached to the nucleaus, which means that they can more easily be attached to the neighboring atoms, creating a negative charge in this atom and leaving the original atom as a positive charged ion. This band is defined as the conduction band, which is responsible for the conduction of electricity and heat. The energy difference between an electron in the valence band and an electron in the innermost shell of the conduction band is called the band gap.

Materials that have a full valence band and an empty conduction band are called insulators, since the energy gap is very large.

When the material has a relatively empty valence band and possibly some electrons in the conduction band, it is called a conductor. As the two bands overlap, the electrons in valence band can accept energy from outside and move to a higher energy level within the same band.

If the material has a partly filled valence band and has average band gaps, it is called a semiconductor. The structures of the bands in semiconductors and insulators are the same, however, semiconductors have a much smaller energy gap.

There are two types of semiconductors. Pure semiconductors are called intrinsic semiconductors and the ones that are slightly impure called extrinsic semiconductors. The valence electrons in intrinsic semiconductors can easily be effected by thermal or optical means and pass the energy gap and move into the conduction band, where they can move freely through the crystal.

The schematic diagrams of the energy bands of these three materials are shown in Figure 3.4.

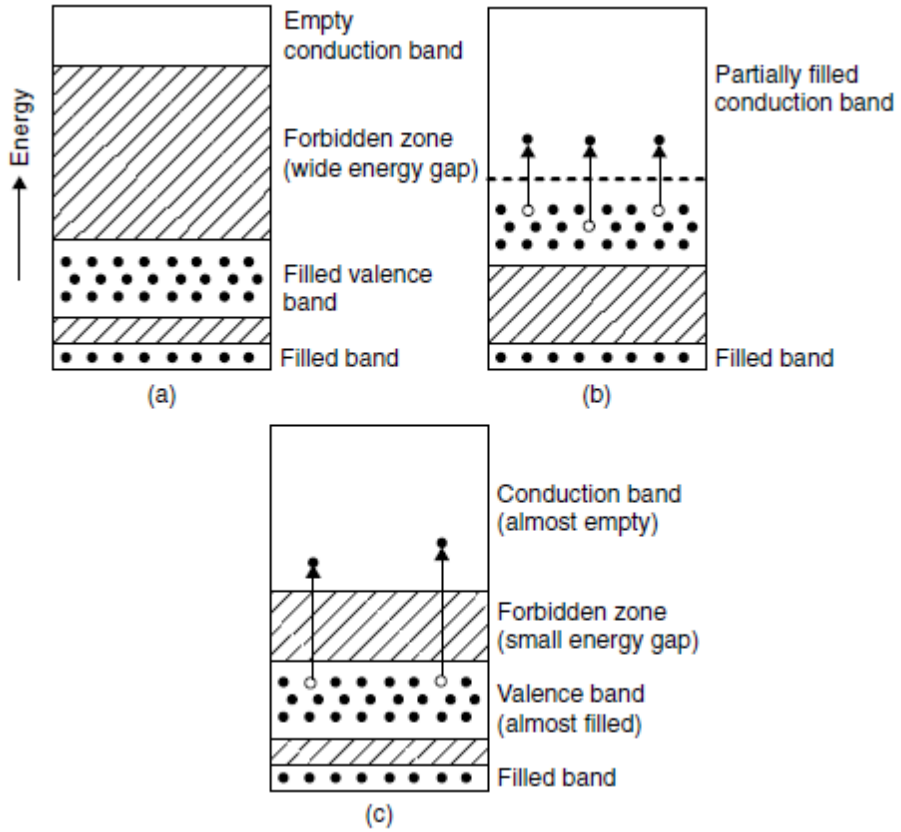

Figure 3.4 The schematic diagrams of energy bands of insulators (a), conductors (b) and semiconductors (c) [8]

3.1.1. p-n Junction

When silicon is combined with a material, if the combined material has more electrons in the valence gap, it is defined as an n-type semiconductor. It has excess electrons that can provide conduction by moving around the crystal, even though it is an electronically neutral material. This can be achieved by replacing Si atoms with periodic table group 5 elements such as arsenic (As) or antimony (Sb).

In the case that the combined material has less electrons in the valence gap, it is defined as a p-type semiconductor. This material is also electronically neutral, however, it has missing electrons in its structure, therefore it can take in the excess electrons. This can be achieved by replacing Si atoms with periodic table group 3 elements such as gallium (Ga) or indium (In). This process forms positive particles, called holes, that can move around the crystal through diffusion or drift. In case the additional electrons fill the holes, the atoms of the combined

material would be negatively charged but fit in the structure more uniformly. Both types of semiconductors are shown schematically in Figure 3.5.

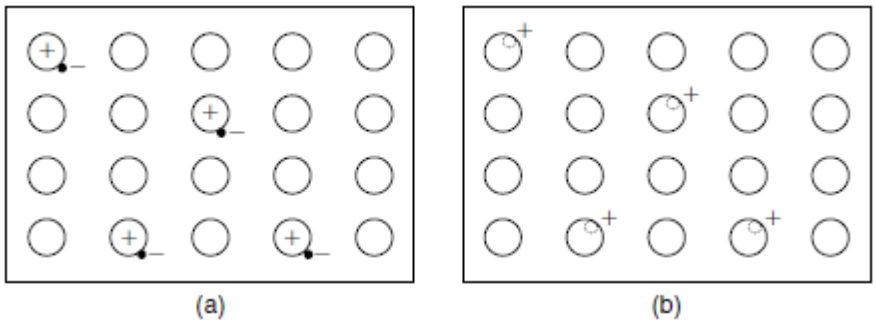

Figure 3.5 Schematic diagrams of (a) n-type and (b) p-type semiconductors [8]

If the two materials are joined together, the excess electrons in the n-type move to the p-type to fill the holes making them negatively charged, and the holes in the p-type diffuse to the n-type, making them positively charged. The negative charges in the p-type limit the movements of additional electrons that comes from the n-type and the additional electrons from the p-type can move easier because of the positive charges at the junction. As a result, the p-n junction works as a diode. Schematic diagram of the p-n juction is shown in Figure 3.6.

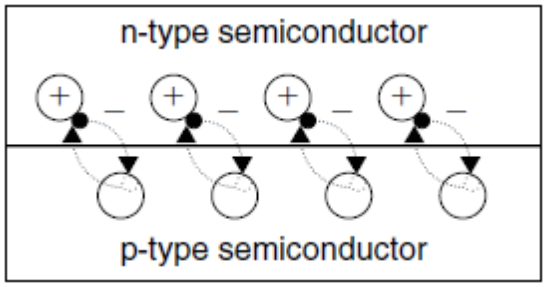

Figure 3.6 Schematic diagrams of the p-n juction [8]

3.2. Photovoltaic Effect

The photon that enters a photovoltaic material can be reflected, absorbed or transmitted through. If the photon is absorbed by a valence electron in the material, the energy of the electron increases. This valence electron can move into the conduction band if the energy of the photon it absorbed is higher than the band gap of the semiconductor. It can move freely in the crystal, which means that it can create a current by flowing through an electric field across the front

and back of the photovoltaic material. If the energy of the absorbed photon is less than the energy of the band gap, the valence electron will not move to the conduction band and the excess energy will be converted into kinetic energy. As a result, the temperature will increase. The reason of the low efficiencies in photovoltaic cells is that only one electron can be freed, regardless of the amount of the energy that absorbed photon contains.

As the electrons and holes diffuse across the p-n junction, they create an electric field across the boundary of the junction. The free electrones are generated in the n-type side by the photons. As the photons strike the surface of a solar cell and are absorbed by the semiconductor, some of them create pairs of electrons and holes. The electric field of the p-n junction separates the charges if these pairs are near the p-n junction. An electric current will flow if the two sides of the solar cell are connected through a load. The operation of a photovoltaic cell is shown in Figure 3.7.

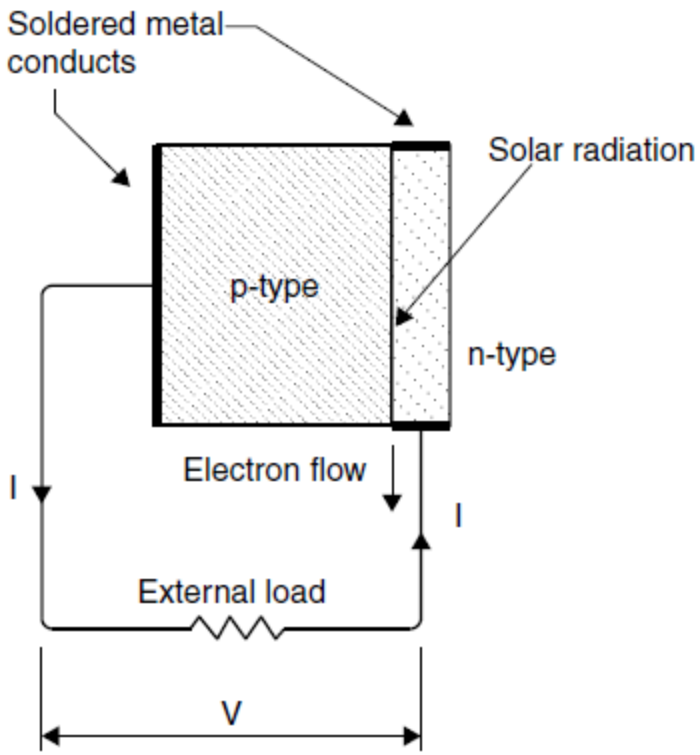

Figure 3.7 The operation of a photovoltaic cell [8]

Photovoltaic cells consist of the photovoltaic material, metal grids, antireflection coatings and supporting material. They are optimized to maximize both the amount of sunlight entering the cell and the power production of the cell [8].

3.3. Photovoltaic Cell Characteristics

The current that is created by capturing the electrons in the photovoltaic cell is called photocurrent, I_{ph}. During the night, the p-n junctions does not produce any current or voltage and solar cell is not active and works as a diode.

In case it is connected to an external voltage supply, it generates a current called the diode or dark current, I_D. A solar cell is usually shown as an electrical equivalent one-diode model, which can be used for a cell, a module of cells or an array consisting of several modules.

This model has a current source which is I_{ph}, one diode, a series resistance, R_S and an internal shunt resistance R_{SH}, as shown in Figure 3.8.

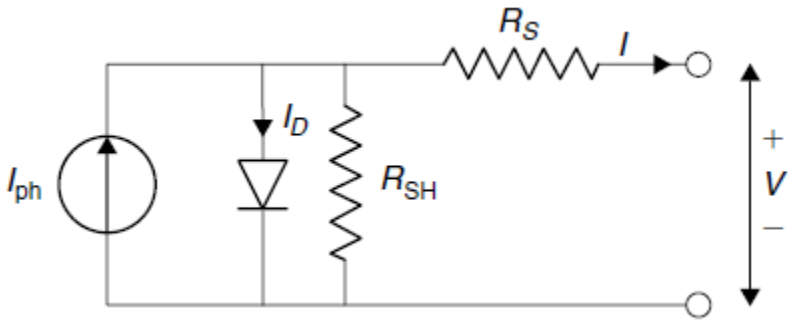

Figure 3.8. Single solar cell model [8]

Since the shunt resistance is usually much bigger than a load resistance while the series resistance is much smaller than a load resistance, less power is dissipated internally within the cell. If these two resistances are ignored, the difference between the photocurrent I_{ph} and the normal diode current I_D is the net current that is given by the formula Eq. 3.1

$$I = I_{ph} - I_D = I_{ph} - I_o\left[\exp\left(\frac{eV}{kT_C}\right) - 1\right] \qquad \text{(Eq. 3.1)}$$

where ;

k = Boltzmann's gas constant, = 1.381 x 10^{-23} J/K.

T_C = absolute temperature of the cell (K).

e = electronic charge = 1.602 x 10^{-19} J/V.

V = voltage imposed across the cell (V).

I_o = dark saturation current, which depends strongly on temperature (A).

Figure 3.9 shows the I-V characteristics of a solar sell for a certain irradiance G_T at a fixed cell temperature T_C. The current in the PV cell depends on the external voltage applied and the amount of sunlight that strikes the cell. The current is maximum when the cell is short-circuited (short-circuit current I_{SC}) and the voltage is 0. If the PV cell circuit is open, with the lead not making a circuit, the voltage is maximum (open-circuit voltage V_{OC}) and the current is 0. At each case, the power (current times voltage) is 0. Between open circuit and short circuit the power output is more than 0. The current-voltage curve in Figure 3.9 shows the range of combinations of current and voltage.

If the terminals of the cell are connected to a variable resistance, R, the intersection of the I-V characteristics of the solar cell and the I-V characteristics of the load determines the operating point. It is shown in Figure 3.9. that, if the load resistance is small, the cell operates in the AB region and if it is large it operates on the DE region. The maximum power is obtained at which point (point C in Figure 3.9) the load resistance is optimum, R_{Opt}, and the maximum power dissipated in the resistive load is given by $P_{max} = I_{max} \times V_{max}$. Therefore, point C in Figure 3.9. is defined as the maximum power point.

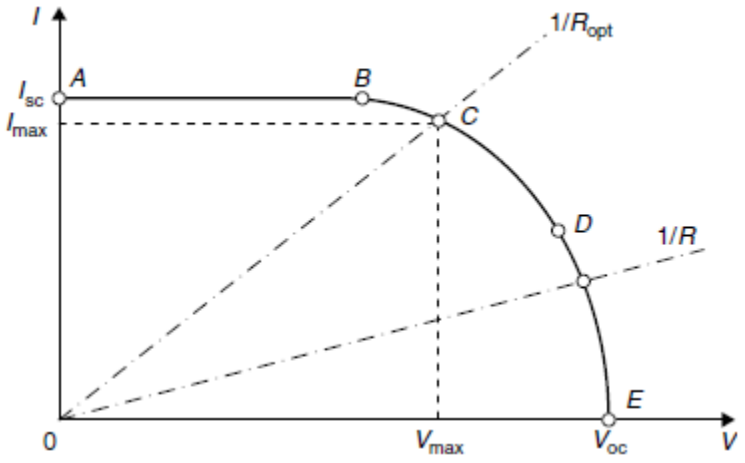

Figure 3.9 Current-voltage curve for photovoltaic cells [8]

Fill factor , FF, is an additional parameter that effects the maximum power. It is a measure of the real I-V characteristics and its value is greater than 0.7 for good solar cells. The fill factor decreases as the cell temperature increases.

Hence, by illuminating and loading a PV cell so that the voltage equals the maximum voltage, V_{max}, the output power is maximized. Resistive loads, electronic loads or batteries can be used to load the cell.

Efficiency of the PV cells is defined as the ratio between the maximum electrical output of the solar cell and the incident light power. Improvements in cell efficiencies result as a reduction of cost in photovoltaic systems. These efficiencies reach up to 12-15% depending on the type of the solar cell in the mass production lines.

Usually, efficiencies are reported under the conditions of constant cell temperature (25 °C) and irradiance (1000W/m2). If the efficiency is calculated for the maximum electrical output at the maximum incident light power, it is defined as the maximum efficiency and calculated as follows (Eq.3.2) :

$$\eta_{max} = \frac{P_{max}}{P_{in}} = \frac{I_{max} V_{max}}{A G_t} \qquad \text{(Eq. 3.2)}$$

where A = cell area (m^2).

Solar cells can be connected in series or paralel. As shown in Figure 3.10 , if two identical cells are connected in parallel, the current is doubled while the voltage remains the same, if the cells are connected in series, the voltage is doubled while the current remains the same.

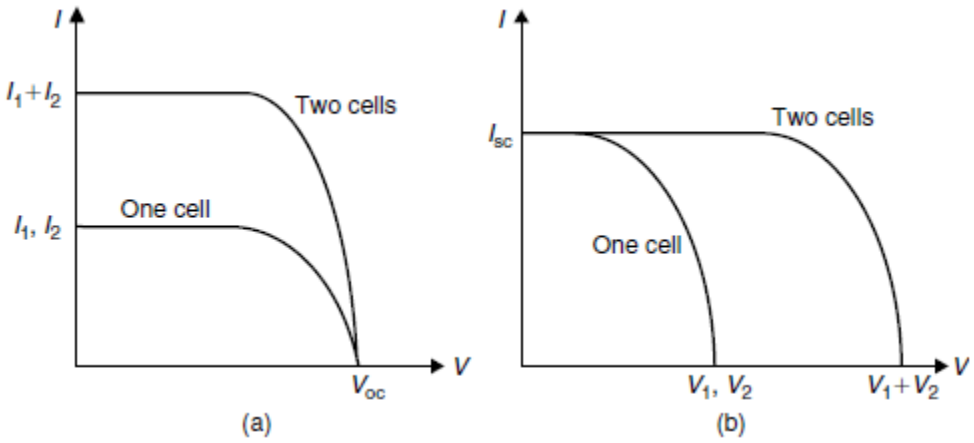

Figure 3.10 Connection of solar cells; (a) parallel connection and (b) series connection [8]

PV cells are fragile and affected by corrosion by humidity or fingerprints. In addition, the operating voltage of a single PV cell is about 0.5V, which is impractical for many applications. Therefore, they are collected as a module to reach usable operating voltages and provide protection. The cells are usually series connected to produce an operating voltage around 14-16V. After that, they are encapsulated with a polymer, a glass cover on the front and a back material, all of which can be designed for harsh environment conditions.

PV modules have different performance characteristics which depend on the type of PV material and the manufacturer. The atomic structure and the composition of the PV material have important effects on system design and performance.

Photovoltaic systems are usually designed as modules that are connected in arrays. Figure 3.11 shows an array with M_P parallel branches each with M_S modules in series.

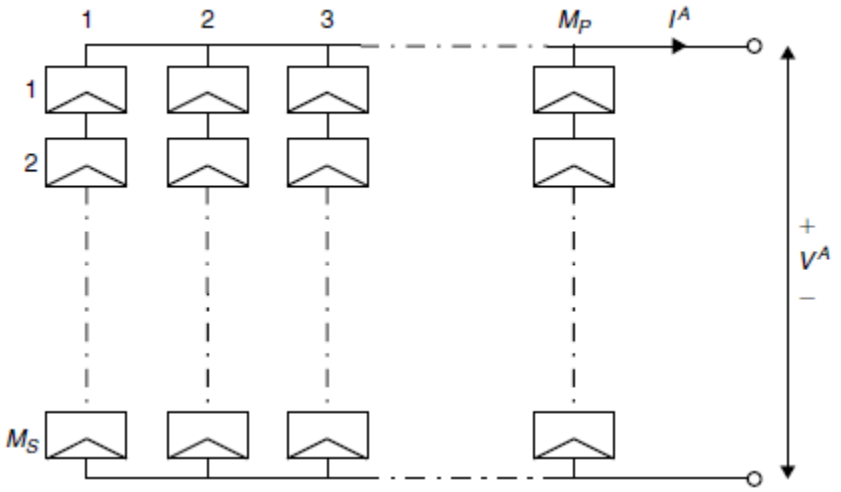

Figure 3.11 PV array that consists of M_P parallel branches each with M_S modules in series

PV cells are effectable by corrosion by humidity or fingerprints and since the operating voltage of a single PV cell is about 0.5 V, which is unusable for mant applications, PV cells are collected in modules to provide usable operating voltages and protection from the environment. Usually cells are series connected to other cells to produce an operating voltage around 14-16 V and they can be designed for specific conditions such as hot, humid, desert or frozen climates. These strings of cells are encapsulated with a polymer, a front glass cover and a back material. Photovoltaically active material in the module has important effects on system design and performance [8].

3.4. Types of PV Technology

Different types of PV technologies are available today.

- Monocrystalline silicon cells : These cells are made from pure monocrystalline silicon which has almost no defects or impurities. The complicated manufacturing process required to produce them makes them more expensive but they can reach high efficiencies, which are around 14-16%.
- Polycristalline silicon cells : These cells are produced using various grains of monocrystalline silicon. They are cheaper to produce than monocrystalline silicon cells due to the simpler manufacturing processes, but they have slightly less efficiencies (around %12).
- Amorphous silicon cells : These cells are composed of silicon atoms in a thin homogenous layer instead of a crystalline structure. They can absorb light more effectively than crystalline silicon cells, so they can be thinner, extremely reducing the photovaltaic material requirements (about 1μm compared to 100μm for crystalline silicon cells). Therefore they are know as thin film PV technology. They are cheaper to produce but they have low efficiencies which are around 6%, and fort his reason they are more suitable for applications that high efficiency is not required and low cost is important.

Promising materials such as cadmium telluride (CdTe) and copper indium diselenide (CIS) are also being used for PV modules. The advantages of these materials are that they can be produced by a relatively inexpensive industrial processes and offer higher efficiencies than amorphous silicon cells.

Nano PV cells are considered the third generation of PV devices and are stil under investigation. They are made by coating or fixing printable and flexible polymer substrates with electrically conductive nanomaterials. This generation of PV cells are expected to be commercially available in the next few years and reduce the highly costs of PV cells [8].

3.5. Inverters

Inverters are used to convert direct current into alternating current electricity. The output of an inverter can be single or three phase and they are rated by the total power capacity, which ranges from hundreds of watts to megawatts. Both type and size of the load should be specified for the inverter that is planned to use.

The inverters are characterized by a power dependent efficiency, η_{inv}. Besides converting DC to AC, the main function of the inverter is to keep a constant voltage on the AC side and conver the input power P_{in} to output power P_{out} with the highest possible efficiency. The formula is (Eq. 3.3) :

$$\eta_{inv} = \frac{P_{out}}{P_{in}} = \frac{V_{ac} I_{ac} \cos(\varphi)}{V_{dc} I_{dc}} \quad \text{(Eq. 3.3)}$$

where

$\cos(\phi)$: power factor.

I_{dc} : current required by the inverter from the dc side, i.e., controller (A).

V_{dc} : input voltage for the inverter from the dc side, i.e., controller (V).

Different types of inverters are commercially available but not all of them are suitable for feeding back the power into the main supply.

The two basic types of PV system applications are stand-alone and grid connected systems. Stand-alone PV systems are used in areas that have no easy access or inaccessable to main electricity grid, so the energy produced is normally stored in batteries.

In grid-connected applications, the system is connected to the local electricity network. Therefore, the electricity that is generated can be used immediately during the day (in office buildings, industrial processes, etc) or be sold to an electricity supply company (for domestic use since the occupier can be out during the day). When the PV system does not generate electricity in the evening, the needed electricity can be bought from the grid. This means that the grid acts as an energy storage system, and as a result there is no need for a battery in the system. Figure 3.12 shows the schematic diagram of a grid connected system.

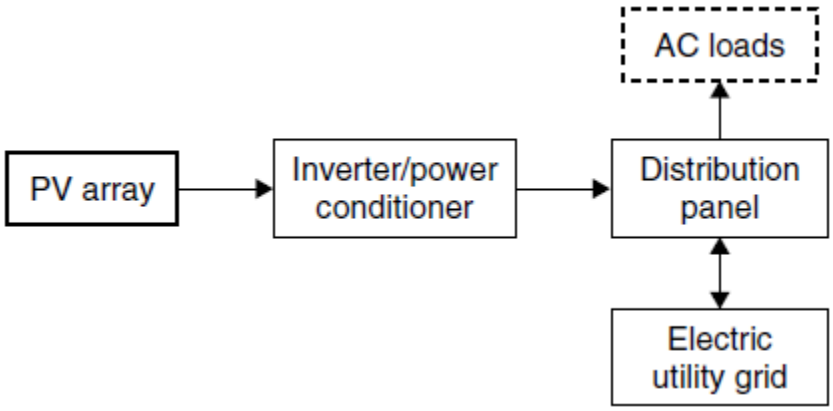

Figure 3.12 Schematic diagram of a grid connected system [8]

4. Chosen Technologies For The Project

The solar energy company that is working on this project is using one PV module type and two different types of inverters according to the project.

The chosen PV modules are manufactured by Korean company Hyundai Heavy Industries. The model is called HIS-S250RG and it is a silicon-type PV module with nominal power of 250 Wp under standard test conditions.

For inverters, the company uses products of German companies Kostal or KACO. These inverters are used for the first part of the simulations and after that different products of ABB, Fronious, Danfoss, SMA, SAMIL are used in simulations for comparison. Models of these inverters are :

- Kostal PIKO 20 kW
- KACO Powador 48.0 TL3 Park M 40kW
- Fronious International Symo 20.0-3-M 20 kW
- ABB Trio-20.0-TL-OUTD 20 kW
- SMA Sunny Tripower 20000 TL-30 20 kW
- Danfoss FLX Pro 15 15 kW
- SAMIL SolarLake 17000TL 17kW

Detailed technical properties of the chosen components are available in Appendix 1.

5. Design of PV System

5.1. PVSyst Software

PVSyst is a computer software which deals with grid-connected, stand-alone, pumping and DC-grid (public transportation) photovoltaic systems, including databases for extensive meteo and PV systems components and general solar energy tools. The user can achieve a comprehensive system design using detailed hourly simulations and can perform different system simulation runs using different parameters and compare them.

Figure 5.1 shows the outline of a project and the parameters that can be modified in PVsyst.

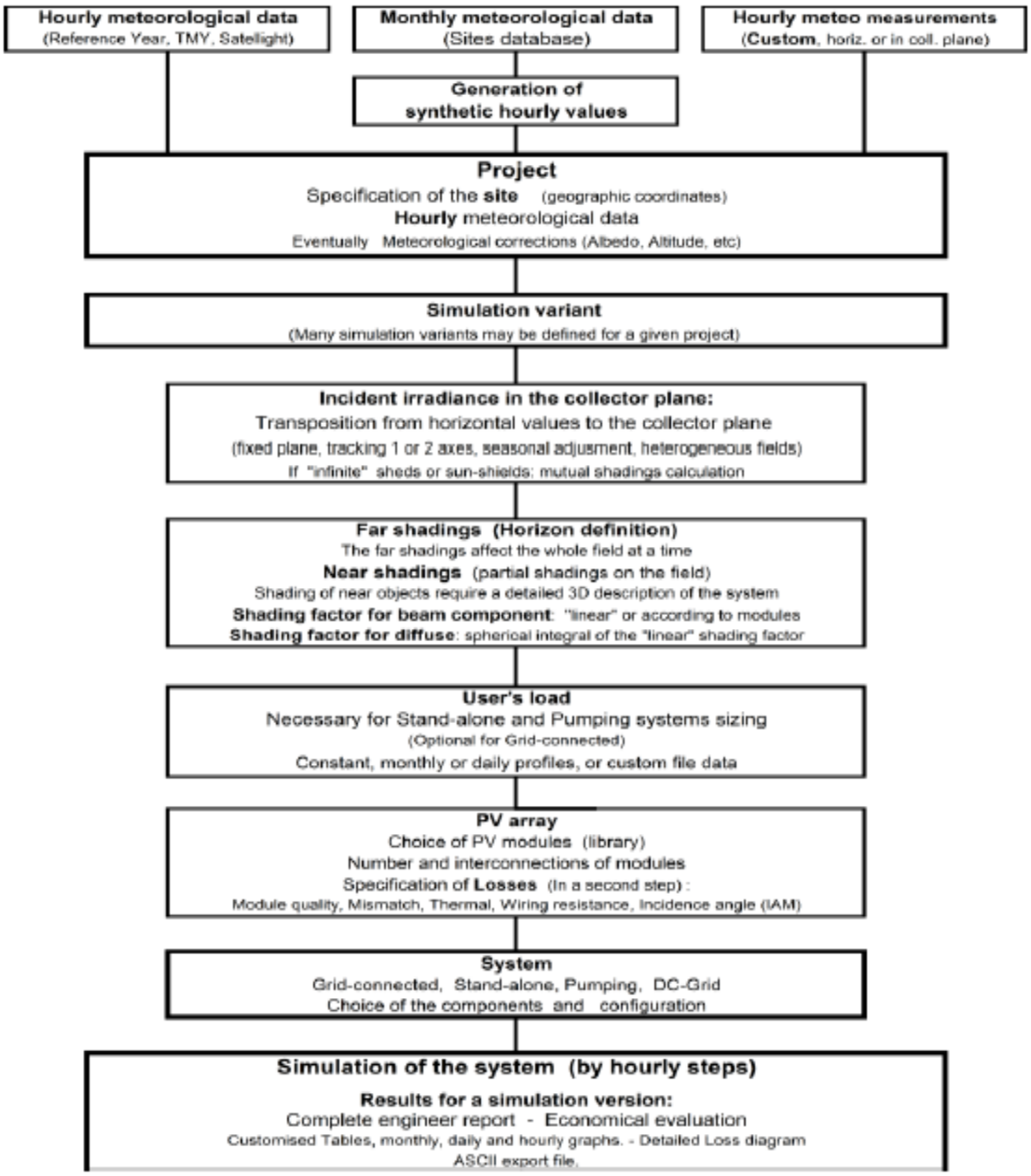

Figure 5.1. Outline of a project and parameters that can be modified in PVSyst [13]

5.2. Site Assessment

Site assessment is one of the most important parts of the design phase. Identifying the available roof areas with south-facing and shade-free surfaces, building orientation, available area for installation and mounting is essential to design the most suitable photovoltaic system.

The site of the project is located in Vitamiini street in Tartu, Estonia. Installation opportunities, possible objects that can cause shading, orientation and dimensions of the building were examined and an initial 3D illustration of the considered PV system was constructed using PVSyst software (Figure 5.2 and 5.3) , after calculating the inter row spacing (which is explained in detail in section 5.5). The azimuth angle of the proposed project was calculated as -7° and used in simulations.

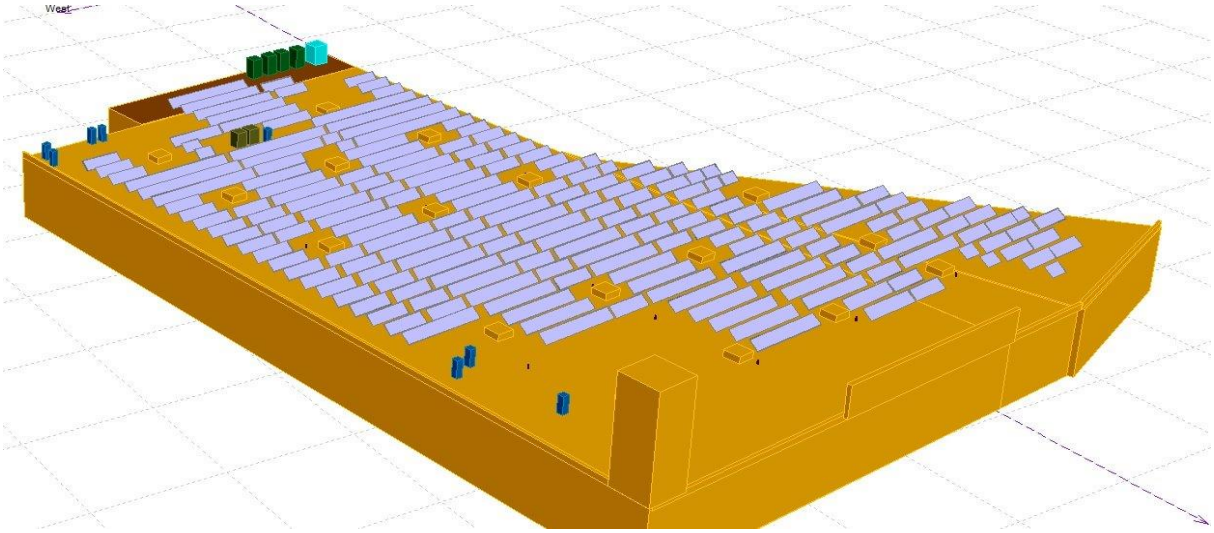

Figure 5.2 3D illustration of the considered PV system

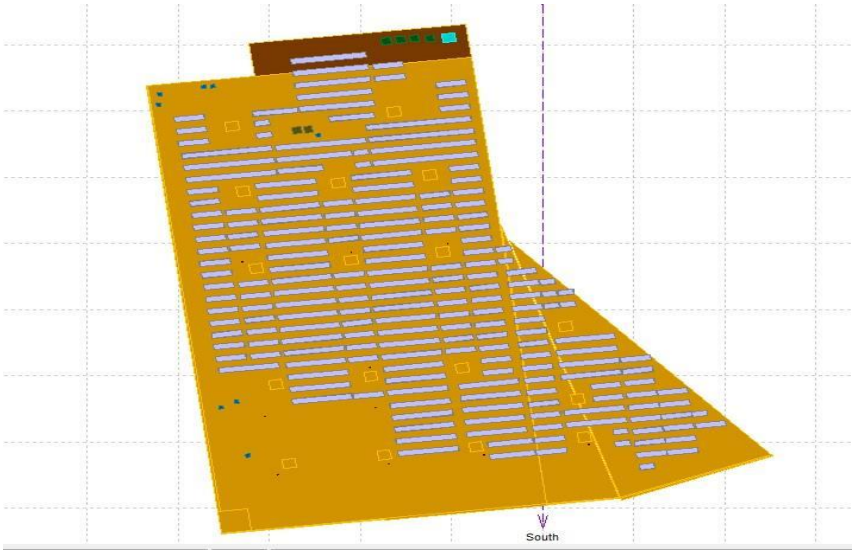

Figure 5.3 3D illustration of the considered PV system

5.3. Meteorological Data

In order to evaluate and optimize photovoltaic systems, it is essential to have a relevant and detailed meteorological data. The accuracy of this data has a decisive effect on selecting the suitable technology and design, as well as determining the economical value of the project [14].

The project in PVSyst starts with selecting the geographical location in order to generate the suitable meteorological data. This also allows the user to interpolate meteorological data for the selected geographical location in case it is not available.

Different varieties of meteorological data is used in PVSyst. These are

- Horizontal global irradiaton
- Average external temperature
- Horizontal diffuse irradiation
- Wind velocity

Meteonorm is the main meteorological data program that is used in PVSyst but it is also possible to use different meteorological databases. Table 5.1 shows the available databases that can be imported to the software.

Database	Region	Values	Source	Period	Variables	Availability	PVsyst import
Meteonorm	Worldwide	Hourly	**Synthetic** generation	1960-1991 and 1995-2000	GHI, DHI, TA VindVel	**Included in PVsyst V 6**	Direct by site choice
Satellight	Europe	Hourly	**Meteosat** Any pixel of about 5x7 km²	5 years **1996-2000**	GlobH **no temper.**	Web free	Direct by file
US TMY2/3	USA	Hourly	NREL, **1020 stations** Typical Meteo Years	**1991-2005** (samples)	GHI, DHI, TA WindVel	Web free	Direct by file
EPW	Canada	Hourly	CWEC, **72 stations** Typical Meteo Years	**1953-1995** (samples)	GHI, DHI, TA WindVel	Web free	Direct by file
ISM-EMPA	Switzerland	Hourly	22 stations Design Ref. Years	**1981-1990** (samples)	GHI, DHI, TA WindVel	Included in PVsyst	Included in database
Solar Anywhere (SUNY model)	USA + Hawaii	Hourly	**Satellites** by 10x8 km²	1998 - today	GlobH, DiffH Temper for pay Wind for pay	Web 2010 - today for pay	Direct by file
Helioclim - 3 (SoDa)	Europe Africa	Hourly	**Meteosat**	**from 02/2004 => today**	GlobH **no temper.**	Web **For pay** 2005 free	Direct by copy/paste or PVsyst format
SolarGIS (Geomodel)	Worldwide	Hourly	**Meteosat, ERA**	**1994 - today**	GHI, DHI, TA	**For pay**	Direct (file) PVsyst format
3Tiers	Worldwide	Hourly	Satellites Spectroradiometer MODIS	**1998 - today**	GHI, DHI DNI available **no temper.**	**For pay**	Direct (file) PVsyst format

Table 5.1 Available meteorological databases for PVSyst [13]

The simulations in PVSyst are run over a year in hourly steps. If there is no specific data for the geographical location, PVSyst generates the required data by using well-established

algorithms and models for irradiance from monthly known values to hourly data, and daily profile parameters for temperature as monthly average, since the PV production will not strongly depend on daily temperature sequences. This is known as synthetic data generation. Figure 5.4 shows the monthly meteorological data generated in PVSyst for Tartu.

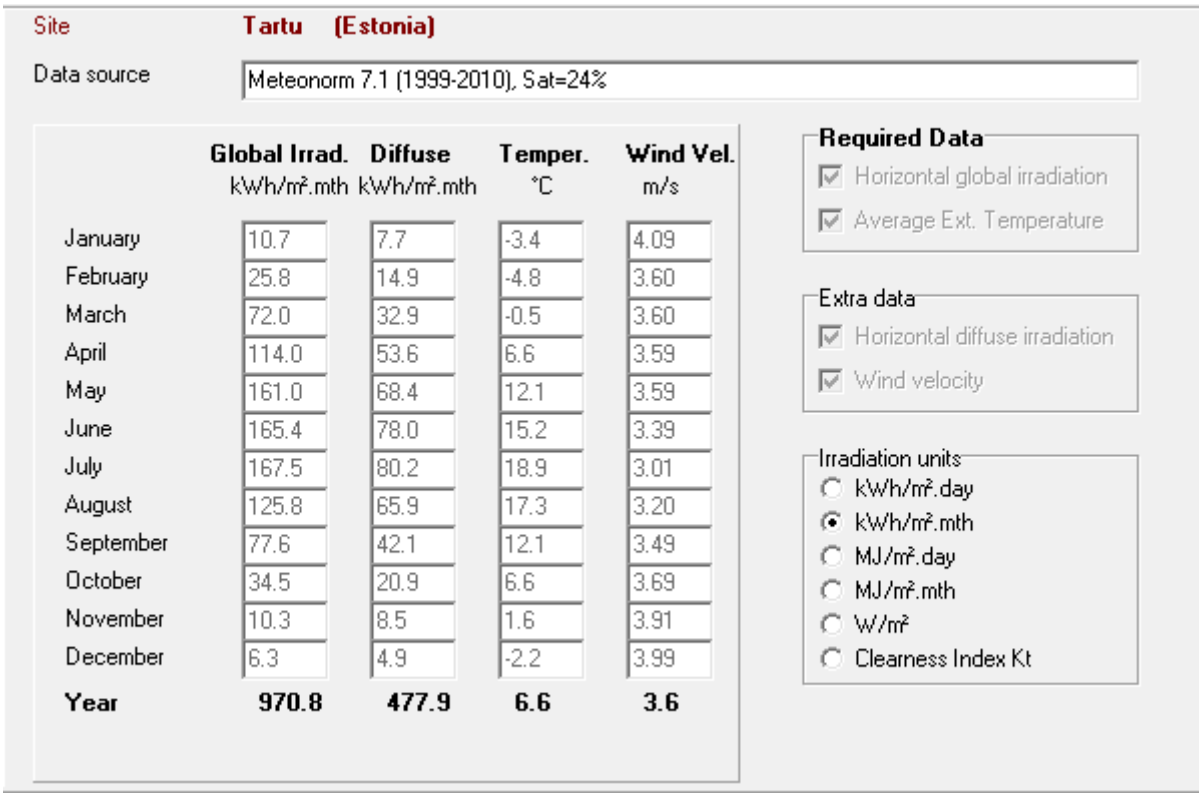

Figure 5.4 Monthly meteorological data generated in PVSyst for Tartu

The albedo coefficient is used to calculate the fraction of global incident irradiation reflected on a tilted plane by the ground. This value is usually taken 0.2 (as default in the software) since the additional albedo calculations are hardly effecting the global incidence irradiation as seen in practice (except for vertical planes). Table 5.2 shows some usual values for albedo factor.

Urban environment	0.14-0.22
Grass	0.15-0.25
Fresh snow	0.82
Wet snow	0.55-0.75
Dry asphalt	0.09-0.15
Concrete	0.25-0.035

Table 5.2 Some albedo values

In case the location has a snowy environment, the albedo value can be chosen as 0.8 for some months. Figure 5.5 shows the chosen albedo values in simulations.

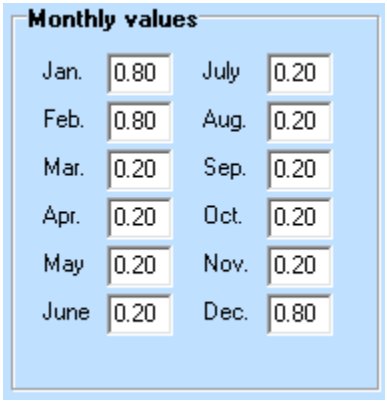

Figure 5.5 Albedo values used in simulations

Changes in module temperature depending on the air temperature and irradiation on the module should also be included into calculations in order to size the PV array voltage according to the inverter properties. The software allows the user to specify these four different site-dependant parameters as reference temperatures.

Maximum array voltage is calculated using the minimum temperature that has ever been measured at the geographical location and known as the lower temperature for absolute voltage limit [13]. The lowest recorded temperature for Tartu is-38.6°C for the past 25 years [15].

Usual operating temperature under 1000 W/m is kept default (50°C) since it is not used for sizing.

Since PV modules recieve a lower level of irradiance and work in a higher temperature than standard test conditions during operations, Nominal Operating Cell Temperature is used to calculate the module temperature in different irradiance and air temperature conditions. Nominal Operating Cell temperature is defined as the stable temperature under the conditions of AM1.5 spectrum at open circuit at an ambient temperature of 20°C, 1 m/s wind speed and G_{NOCT}=800 W/m^2 irradiance. Equation 5.1 [16] is used to calculate the module temperature T_M

$$T_m = T_a + \frac{(NOCT-20)\times G_M}{G_{NOCT}} \quad \text{(Eq. 5.1.)}$$

where T_A is the ambient temperature, is the G_{NOCT} irradiance and G_M is the irradiance on the solar module. According to the data provided by PVSyst and the Eq. 5.2, the values for winter and summer operating temperature are 1°C and 67°C, respectively. These parameters are only used in the design process and not used for the simulations and are shown in Figure 5.6.

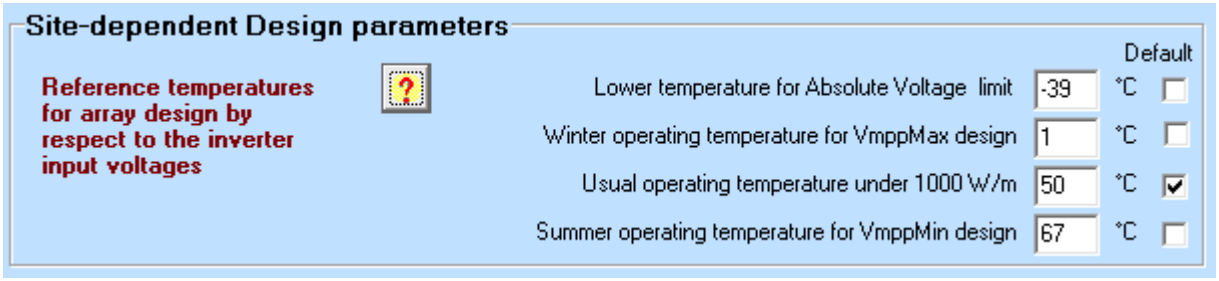

Figure 5.6 Site-dependent desing parameters

5.4. Orientation Optimization in PVSyst

PVSyst software uses a tool to calculate the best possible orientation for a PV system. The transposition factor is used to calcuate the ratio of incident irradiation on the plane, to the horizontal irradiation, which can increase or decrease the output depending on the tilt of the collector plane.

Hourly meteo data is used to calculate the transposition factor and it is also possible to choose the optimizing period. Since the summer optimization generally has a flat optimum, the designer has the flexibility in changing the orientation without much decrease in the output, as it is common when the tilt is low.

Table 5.3. shows the yearly total global incident irradiation in the collector plane for Tartu according to the tilt angles.

Tilt Angle (°)	Total Global Incident Irradiaton (kWh/m^2/y)
35	1173.7
36	1175.0
37	1176.1
38	1176.9
39	1177.5
40	1177.9
41	1178.1
42	1178.0
43	1177.6
44	1176.9
45	1176.0

Table 5.3. Yearly total global incident irradiation in the collector plane for Tartu according to the tilt angles

As seen in the table, the best possible angle for total global incident irradiation in the collector plane in Tartu is 41° .

5.5. Inter row spacing

The tilt angle and the spacing between the modules can effect the amount of shading on a ground-mounted system. Total available area can be increased and shading losses can be decreased by optimization of the tilt angles and space between the module rows [17].

Inter-row spacing for the PV system can be calculated according to module width, module tilt angle and position of the Sun using Eq. 5.2. [18]

$$D = \left[(W \cos \beta) + \left(\frac{W \sin \beta \cos \gamma_S}{\tan h_S}\right)\right] \quad \text{(Eq. 5.2.)}$$

where D is the distance between rows, W is the width of modules, β is module tilt angle, γ_s is the solar azimuth and h_s is the solar altitude.

Module rows are dimensioned with respect to the equinoxes, which represents the time when the front rows should not be shading the rows behind them. The distance was calculated according to the spring equinox (21st of March) regarding the position of the sun in given hours. Table 5.4. shows the calcuated distances between rows.

Hours	Azimuth γ_s (°)	Altitude h_s (°)	Distance between rows (m)
09.00	-55	20	1.785
10.00	-40	26	1.782
11.00	-23	30	1.797
12.00	-6	32	1.795

Table 5.4. Calculated distances between rows

According to the calculations, 1.8 m used as the distance between rows in the simulations. In commercial rooftop systems, tilt angles of the modules are lowered in order to increase the available system area. Extra space needed to eliminate shading loss due to the distance between rows is usually not practical [18].

5.6. Shading

In PVSyst software, the shadings are categorized in two : far shadings and near shadings.

Far shadings are defined as the shadings from an object that is adequately far away from the PV system. The area between these objects and the PV system can be considered as ten times the PV field size.

Near shadings are defined as the detectable shades on the PV field that is caused by near objects. Therefore a detailed 3D description of the PV system and its environment is essential for the treatment of near shadings.

Two kinds of losses are examined for the beam component of near shadings.

Irradiance losses (linear shading losses) are defined as the shortfall of irradiance on the cell [13].

Electrical losses are defined as the decrease in current caused by the shadings on the cell area. When the cells and modules are connected in series, the maximum current going through the series is the limited to the lowest current. This will result in a discrepancy in the series and can lead to hot-spot heating, since the uneffected cells will produce higher voltages because the shaded cell decreases the current for the uneffected cells, leading to over-heating which can damage the modules. Over-heating can be prevented by using bypass diodes which limit the increasement of higher voltages in the reverse-biased direction by redirecting the current. Figure 5.7 shows the characteristic I-V curves of a module with 36 cells where one cell is %75 shaded [5].

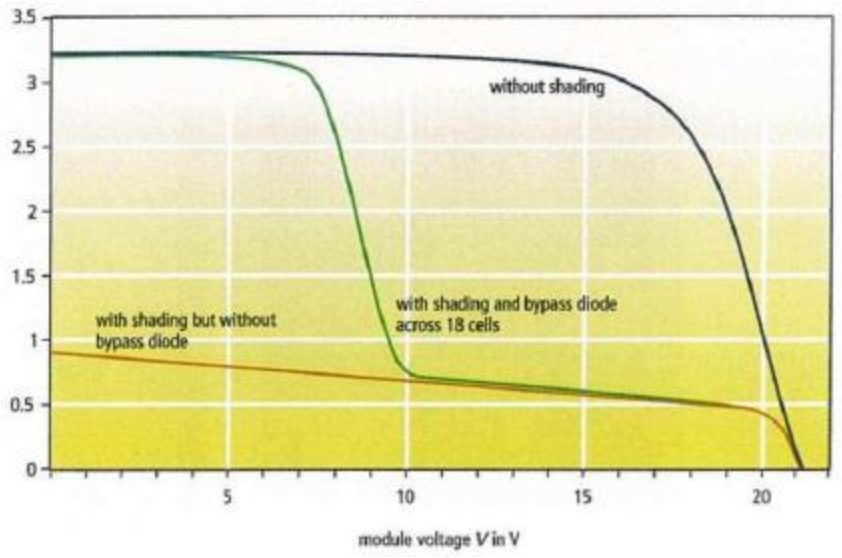

Figure 5.7 Characteristic I-V curves of a module with and without bypass diodes

The electricity production changes to a non-linear state when there is a shaded PV cell on the string, which hardly engages in the production even with a bypass diode. PVSyst uses a simplified method of dividing the PV area into strings of modules in series. Then the fraction of electrical effect parameter can be used to define the magnitude of the real effect of partially shaded strings on the electrical production. This can be chosen %100 if the shades are very regular, but if they are more distributed (when there are chimneys and far buildings near the PV system) it can be chosen between %60-80. It was chosen as %70 for the simulations.

5.7. Inverter/Array Sizing in PVSyst

Technical specifications of the inverters is essential to define the sizing of the inverters. The power class, voltage level and the numbers of inverters are regulated by the system and the connection concept of the system [5].

Many inverter producers suggest a PV array nominal power (P_{NomDC}) limit or a fixed ratio of inverter nominal output (P_{NomAC}) to P_{NomDC} of 1.0 to 1.1 . Depending on the temperature of the device, many inverters accept a part of overload for a short period. But since P_{NomDC} is defined under standard test conditions, this value is very rarely or never reached.

On the other hand, oversizing the inverter will lead to a decrease in efficiency, since the inverter will perform on its low power range more frequently.

The sizing principle that is used in PVSyst is based on an acceptable overload loss during operation. As a result, it involves estimations or simulations in the actual conditions of the system, such as meteo, orientation and losses.

All the modern inverters are capable of changing the operating point in the I-V curve of the PV array in case the maximum power of the array exceeds its P_{NomDC} limit. Thus, the inverter will not take any overload but the potential power of the array will not be attained, meaning that there will not be any power dissipation or overheating.When the power of the inverter is slightly under the maximum power reached by the array in real operation, there is a very little decrease in power production. Therefore, the simulation and the examination of the overload loss is a reliable method for determining the size of an inverter.

The sizing principle of PVSyst is specified as :

- 3% > Overload Loss > 0.2% : inverter slightly undersized
- Overload loss > 3%: inverter strongly undersized, prevents the simulation

This is equivalent to a P_{NomDC} / P_{NomAC} order of 1.25 to 1.3 for successfully adjusted systems in practice [13].

5.8. Cable sizing

In order to keep the voltage under a determined loss limit, DC cable sizings are calculated. Suitable cable material and cross section area of the cables are the main parameters used in calculations of cable sizing.

Unfortunately, cable sizing calculations in PVSyst software are not done clearly. Only DC cables are sized with an approximate approach in this study. Figure 5.8 shows the values that are used in simulations.

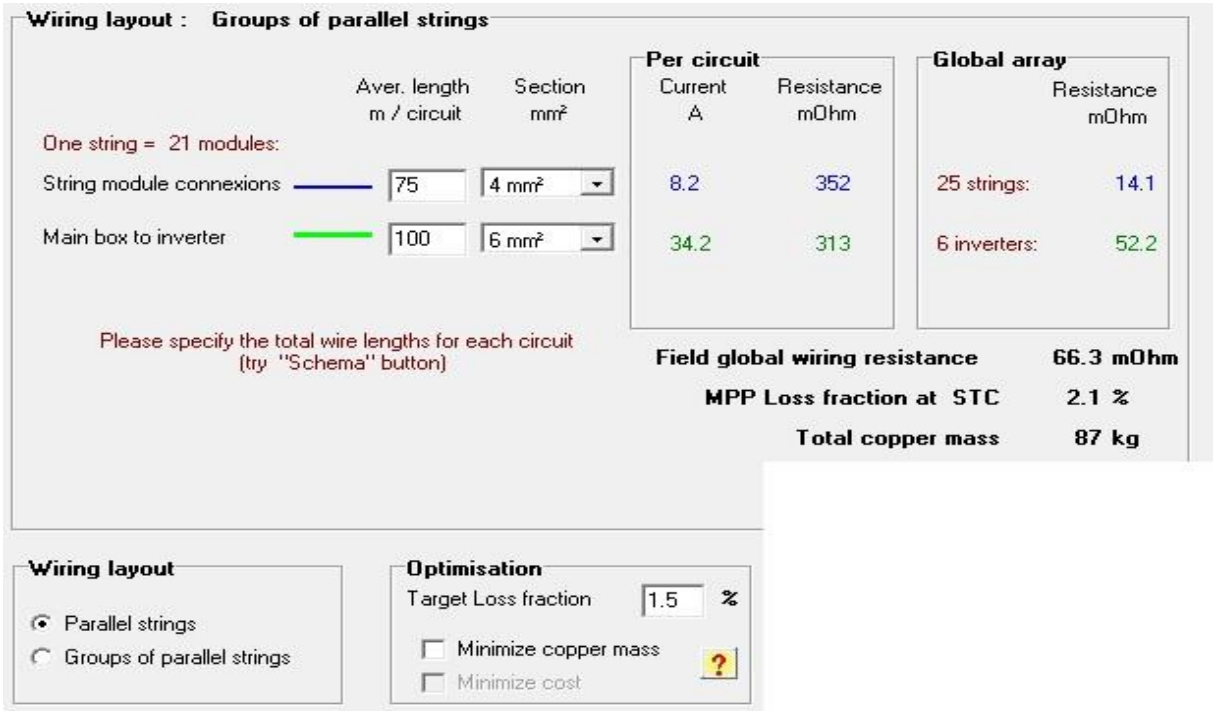

Figure 5.8 Cable sizing parameters used in simulations

5.9. Array Losses

Array losses can be defined as all possible occurrances that decrease the usable array output energy with reference to the PV module nominal power under standard test conditions.

After taking irradiation shadings into account, it is assumed that the ideal PV array will produce 1 kWh energy under 1 kWh irradiance for each installed kWp. This yield is lowered by the following losses:

- Shading Losses : Irradiance deficit and electrical effect (see section 5.6)
- Incidence Angle Modifier (IAM) : The loss of irradiance reaching to the surface of the PV cell due to reflexions increasing with the incidence angle, concerning the irradiance under normal incidence. PVSyst uses the ASHRAE model for parametrisation, which depends on only one parameter. Default value (0.05) of this parameter which is defined by the software is used in simulations.
- Thermal behaviour of the PV array : Defined as an energy balance between the ambient temperature and the increase in module temperature according to the incidence irradiance. PVsyst uses the following equation (Eq. 5.3) :

$$U.(T_m - T_a) = \alpha.G_M.(1-\eta) \quad \text{(Eq. 5.3)}$$

where α is the absorption coefficient of the solar radiation, which is determined as 0.9 as the usual value. η is the PV efficiency with respect to the module area, which is calculated according to the operating conditions by PVSyst when possible, otherwise it is taken as %10 as default.

U is the thermal loss factor which characterizes the thermal behaviour and defined as the following equation (Eq. 5.4)

$$U = U_c + U_v . v \quad \text{(Eq. 5.4)}$$

where U_C is the constant component and U_V is a factor corresponding to the wind velocity V. These factors are effected by the mounting of the system and the reliability of the measured data (such as wind velocity).

- Real module performance : This parameter defines the decrement in average module quality (efficiency) according to the specifications of the manufacturer [13]. The optimal value for this parameter is defined as %0.7 [19].
- Mismatch losses : The slight difference of I-V characteristics between the modules in an array results in mismatch losses since the lowest current defines the current of the string. PVsyst software has a tool to calculate the corresponding power loss. This tool first generates a statistical sample of modules, setting V_{CO} and I_{SC} values with respect to a gaussian or square distribution, adds the I-V characteristics of each module in each string (add voltages) and gathers the strings in the array (add currents). Lastly, it draws the resulting I/V curve of the array, and identifies the MPP value which may be compared to the MPP value of an array with identical modules.

  Since each statistical sample has a different result, the software generates an estimated probability distribution, histogram, of the power loss values with different samples. This helps estimate the Mismatch Loss parameter, which has to be defined by the user as an input parameter, and is constant during the detailed simulation. PVSyst suggest the default value of 2% for P_{MPP} .

- Ohmic wiring loss : The wiring ohmic resistance causes losses between the available power from the modules and at the terminals of the array. It can be characterised by a resistance parameter R determined for the global array.
- Light Induced Degradation (LID) loss : In the first hours of exposition to sun, the performance of crystalline modules is reduced with respect to the manufacturer's final tests at standard test conditions, which leads to a loss. This loss is related to the quality of the wafer manufacturing and could be defined from %1 to %3. The default value of LID loss in PVSyst is %2 and used in simulations.
- Soiling losses : Accretion of any kind of dirt (dust, snow, etc.) results losses which is defined as soiling losses. Even though its effects are uncertain and strongly depend on the environment, a great number of studies helps the designer to estimate the value of this factor [20]. Considering average number of days with snow in Tartu, soiling factors for each month is defined in PVSyst, as seen in Table 7.3.

- Irradiance loss : The efficiency of the modules decrease comparing to standard test conditions when the irradiance is low, which leads to irradiance loss. It is a result of the peculiar behaviour of the PV modules, which is described by the one-diode model. In this model, the efficiency at low irradiance depends on two parameters:
    - Shunt resistance exponential behavior (R_{SHUNT}) : R_{SHUNT} increases exponentially when the irradiance decreases. Lower R_{SHUNT} at standard test conditions results in higher efficiency for low irradiances.
    - Series resistance (R_{SERIE}) : Series resistance increase with power and when its higher, the losses at standard test conditions are higher as well.

  Thus, the modules that has low R_{SHUNT} and high R_{SERIE} performs better under low irradiance conditions, comparing to standard test conditions specifications [13].

6. System Performance

In order to compare the performances of different PV systems, derived parameters related to systems energy equilibrium and performance are used in PVSyst software as normalized indicators according to IEC 61724 Photovoltaic System Performance Monitoring – Guidelines for Measurement, Data Exchange and Analysis norms [19].

These indicators are normalized according to array nominal installed power (P_{NOM}) under standard test conditions with regards to incident energy in the collector plane. Thus, they do not depend on the array size, geographical situation or field orientation [13]. This means that two differently configured and located PV systems can easily be compared by analyzing these normalized system performance indices such as yields and losses. Yields are the energy quantities normalized according to the rated array power and the losses are the differences between these yields [19]

The yield energies are defined as a unit of kWh/kWp/day , therefore the quantities are equal to the corresponding operating time under a constant irradiance of 1 kW/m^2 so they can also be defined as a unit of $kWh/m^2/day$.

6.1. Reference System Yield

Reference system yield represents (Y_R) the ideal array yield under standard test conditions with respect to P_{NOM} without any loss. In other words, it is “the number of hours per day during which the solar radiation would need to be at reference irradiance levels in order to contribute the same incident energy as was monitored (19).” Therefore it is numerically equal to the incident irradiance on the array plane and defined as a unit of $kWh/m^2/day$ in PVSyst [13].

6.2. Array Yield

Array yield (Y_A)represents the daily array output energy with respect to the nominal power. In other words, it is "the number of hours per day that the array would need to operate at its rated output power to contribute the same daily array energy to the system as was monitored [19]." It is defined as a unit of kWh/kWp/day in PVSyst.

6.3. System Yield

System yield (Y_F) represents the daily beneficial energy with respect to the nominal power. In other words, it is "the number of hours per day that the array would need to operate at its rated output power to equal its monitored contribution to the net daily load." [19]. It is also defined as a unit of kWh/kWp/day in PVSyst.

6.4. Collection Loss

Collection loss (L_C) respresents the losses due to array operation that are explained in section 5.9 and all other inefficiencies. It is calculated by substracting array yield Y_A from reference system yield Y_R .

6.5. System Loss

System loss (L_S) represents the difference between array yield (Y_A) and system yield (Y_F), which includes the inverter loss in grid-connected systems [13].

6.6. Performance Ratio

Performance ratio (PR) represents the global system efficiency with respect to the nominal installed power and the incident energy. In other words, this ratio "indicates the overall effect of losses on the array's rated output due to array temperature, incomplete utilisation of the irradiation, and system component inefficiencies or failures [19] IEC and calculated by dividing system yield by reference system yield (Eq. 5.6.1.) , therefore it is dimensionless.

$$Y_F / Y_R \qquad \text{(Eq. 5.6.1.)}$$

It is considered as a common way to evaluate PV systems. Usual values for PR are around %60-75 but higher values can be achieved [21].

7. Simulations and Results

Simulations were performed using PVSyst after carrying out a detailed study and analysis of the project. Main simulation parameters were decided according to the softwares recommendations and different designs are compared by tilt angles, two different inverter combinations system losses and performance. After deciding the best possible design, different combinations of more inverters are suggested and compared to the design of the company.

Classification of the first part of the simulations are shown in Table 7.1.

Inverter			
Kostal		KACO	
Simulation Name	Tilt Angle	Simulation Name	Tilt Angle
Kostal 1	16	KACO 1	16
Kostal 2	17	KACO 2	17
Kostal 3	18	KACO 3	18
Kostal 4	19	KACO 4	19
Kostal 5	20	KACO 5	20
Kostal 6	21	KACO 6	21
Kostal 7	22	KACO 7	22
Kostal 8	23	KACO 8	23
Kostal 9	24	KACO 9	24
Kostal 10	25	KACO 10	25
Kostal 11	26	KACO 11	26

Table 7.1 Classification of the first part of the simulations

Since the total number of modules is constant due to the site conditions, total number of modules in series and total number of strings in modules are chosen the same in each simulation. Table 7.2 shows the array design parameters and number of inverters.

	Kostal	KACO
Total number of modules	525	525
Total number of modules in series	21	21
Total number of strings in modules	25	25
Total number of inverters	6	3

Table 7.2 Array design parameters and number of inverters for the first part of the simulations

7.1. Simulation Parameters

Fixed simulation parameters are shown in Table 7.3 , Table 7.4 , Table 7.5 and Table 7.6.

Field type	Fixed tilted plane
Azimuth	-7°
Plane Tilt	16° , 17°, 18°, 19°, 20°, 21°, 22°, 23°, 24°, 25°, 26°
Inter-row spacing	1.8m

Table 7.3 Orientation parameters

Module Quality Loss	%1.5
Light Induced Degradation	%2
Module Array Mismatch Loss	%1

Table 7.4 Module Loss Parameters

January	February	March	April	May	June
%20	%20	%2	%2	%2	%2
July	August	September	October	November	December
%2	%2	%2	%2	%2	%20

Table 7.5 Soiling Loss Parameters

Fraction of electrical effect	%70

Table 7.6 Shading Loss Parameter (electrical)

Table 7.7 and Table 7.8 shows the calculated system losses according to each simulation.

	Kostal										
Simulation Number	1	2	3	4	5	6	7	8	9	10	11
Tilt Angle	16	17	18	19	20	21	22	23	24	25	26
Near Shading (Irradiance Loss)	2.6	2.8	3.1	3.3	3.6	3.8	4.1	4.4	4.7	5.0	5.2
IAM factor on global	3.7	3.7	3.6	3.6	3.5	3.5	3.4	3.4	3.3	3.3	3.3
Soiling loss factor	2.9	2.9	2.9	2.9	2.9	3.0	3.0	3.0	3.0	3.0	3.0
PV Loss due to irradiance level	1.7	1.7	1.6	1.6	1.6	1.6	1.6	1.6	1.6	1.6	1.6
PV Loss due to temperature	0.9	0.9	1.0	1.0	1.0	1.1	1.1	1.1	1.1	1.2	1.2
Shading loss (electrical)	0.9	1.1	1.2	1.3	1.6	1.9	2.1	2.2	2.3	2.4	2.5
Module quality loss	1.5	1.5	1.5	1.5	1.5	1.5	1.5	1.5	1.5	1.5	1.5
LID	2.0	2.0	2.0	2.0	2.0	2.0	2.0	2.0	2.0	2.0	2.0
Mismatch loss	1.0	1.0	1.0	1.0	1.0	1.0	1.0	1.0	1.0	1.0	1.0
Ohmic wiring loss	0.7	0.7	0.7	0.7	0.7	0.9	0.9	0.7	0.7	0.8	0.8
Inverter loss	3.0	3.0	3.0	3.0	3.0	3.0	3.0	3.0	3.1	3.1	3.1

Table 7.7 Calculated system losses (Kostal)

	KACO										
Simulation Number	1	2	3	4	5	6	7	8	9	10	11
Tilt Angle	16	17	18	19	20	21	22	23	24	25	26
Near Shading (Irradiance Loss)	2.6	2.8	3.1	3.3	3.6	3.8	4.1	4.4	4.7	5.0	5.2
IAM factor on global	3.7	3.7	3.6	3.6	3.5	3.5	3.4	3.4	3.3	3.3	3.3
Soiling loss factor	2.9	2.9	2.9	2.9	2.9	3.0	3.0	3.0	3.0	3.0	3.0
PV Loss due to irradiance level	1.7	1.7	1.6	1.6	1.6	1.6	1.6	1.6	1.6	1.6	1.6
PV Loss due to temperature	0.9	0.9	1.0	1.0	1.0	1.1	1.1	1.1	1.1	1.2	1.2
Shading loss (electrical)	0.9	1.1	1.2	1.3	1.6	1.9	2.1	2.2	2.3	2.4	2.5
Module quality loss	1.5	1.5	1.5	1.5	1.5	1.5	1.5	1.5	1.5	1.5	1.5
LID	2.0	2.0	2.0	2.0	2.0	2.0	2.0	2.0	2.0	2.0	2.0
Mismatch loss	1.0	1.0	1.0	1.0	1.0	1.0	1.0	1.0	1.0	1.0	1.0
Ohmic wiring loss	0.7	0.7	0.7	0.7	0.7	0.7	0.7	0.7	0.8	0.8	0.8
Inverter loss	2.1	2.1	2.1	2.2	2.2	2.1	2.1	2.1	2.1	2.1	2.2

Table 7.8 Calculated system losses (KACO)

7.2. Simulation Results

Table 7.9 and Table 7.10 shows the production results according to each simulations

Simulation Name	Tilt Angle	Produced Energy (MWh/year)	Specific Production (kWh/kWp/year)	Performance Ratio
Kostal 1	16	116.8	890	0.810
Kostal 2	17	117.1	892	0.807
Kostal 3	18	117.3	894	0.804
Kostal 4	19	117.5	896	0.802
Kostal 5	20	117.5	895	0.798
Kostal 6	21	117.2	893	0.792
Kostal 7	22	117.3	894	0.789
Kostal 8	23	117.3	894	0.786
Kostal 9	24	117.3	894	0.783
Kostal 10	25	117.3	894	0.780
Kostal 11	26	117.2	893	0.777

Table 7.9 Production results of the simulations (Kostal)

Simulation Name	Tilt Angle	Produced Energy (MWh/year)	Specific Production (kWh/kWp/year)	Performance Ratio
KACO 1	16	117.9	898	0.818
KACO 2	17	118.2	900	0.815
KACO 3	18	118.4	902	0.812
KACO 4	19	118.6	904	0.809
KACO 5	20	118.5	904	0.805

KACO 6	21	118.5	903	0.801
KACO 7	22	118.4	900	0.794
KACO 8	23	118.4	899	0.790
KACO 9	24	118.4	902	0.790
KACO 10	25	118.0	902	0.787
KACO 11	26	118.3	902	0.784

Table 7.10 Production results of the simulations (KACO)

As seen from Table 7.9 and Table 7.10 , the best electricity production results were achieved for the tilt angle 19° . Using this tilt angle and the same simulation parameters, five different inverters manifactured by Fronious, ABB, SMA, Danfoss and SAMIL are chosen to investigate if better results can be achieved. Array design parameters are chosen the same as the first part of the simulations. Table 7.11 shows the array design parameters and number of inverters of the second part of the simulations.

	Fronious	ABB	SMA	Danfoss	SAMIL
Total number of modules	525	525	525	525	525
Total number of modules in series	21	21	21	21	21
Total number of strings in modules	25	25	25	25	25
Total number of inverters	6	6	6	8	7

Table 7.11 Array design parameters and number of inverters for the first part of the simulations

Table 7.12 shows the production results of the second part of the simulations.

Inverter	Produced Energy (MWh/year)	Specific Production (kWh/kWp/year)	Performance Ratio
Kostal PIKO 20 kW	117.5	896	0.802
KACO Powador 48.0 TL3 Park M 40kW	118.6	904	0.809
Fronious Symo 20.0-3-M 20 kW	118.2	901	0.806
ABB Trio-20.0-TL-OUTD 20 kW	118.6	903	0.809
SMA Sunny Tripower 20000 TL-30 20 kW	118.3	902	0.807
Danfoss FLX Pro 15 15 kW	117.7	896	0.803
SAMIL SolarLake 17000TL 17kW	117.5	895	0.801

Table 7.12 Production results of the second part of the simulations

As seen in Table 7.12 , the energy production results and performance ratios are similar to each other, taking into account that most modern inverters convert DC power to AC power with an efficiency of %90 or more most of the time when they are properly sized, but it is

possible to achieve minor improvements. Considering that the project was carried out by the company using Kostal PIKO 20 kW inverter and a fixed mounting system with a tilt angle of 21° , the PV system of the project can be considered as optimized.

A more detailed 3D illustration of the chosen system was constructed according to the results of the simulation using SketchUp 3D illustration software (Figure 7.1.)

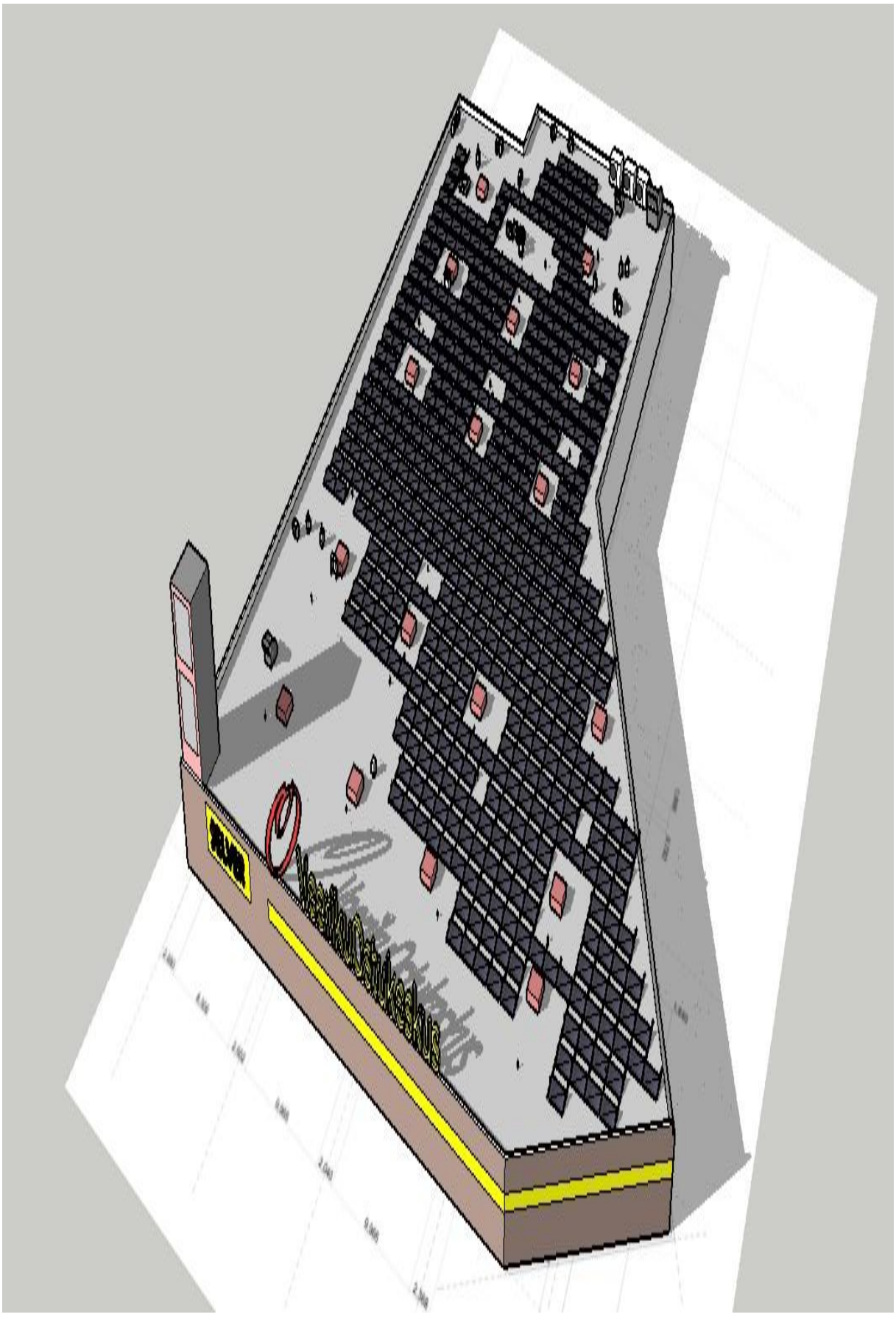

Figure 7.1. Detailed 3D illustration of the chosen system

8. Economic Evaluation

Simple payback time method is used to evaluate the economics of the designed systems. It takes the initial investment costs and the value of yearly electricity production into account to calculate the amount of time to recover the inital investment [22].

It is used as a primary estimation method as it does not include the time value of money or the cash flows. Simple payback times of the systems are calculated according to Eq. 8.1.

$$Simple\ Payback\ Time = \frac{Project\ Initial\ Investment}{Yearly\ Energy\ Sold} \qquad \text{(Eq. 8.1.)}$$

In order to calculate the simple payback times, total investment of the systems are calculated according to the prices that are given from the retailers to the company. Table 8.1 shows the prices of the chosen systems components. Other costs concerning the cables, transportation, labor etc. is calculated according to price per Wp which is 131 kWp for each system.

PV Module	Number of PV Modules	Price per PV Module	Total Cost of PV Modules
Hyundai HIS-S250RG	525	185	97125
Inverter	Number of Inverters	Price per Inverter	Total Cost of Inverters
Kostal PIKO 20 kW	6	2450.2	14701.2
KACO Powador 48.0 TL3 Park M 40kW	3	4818.8	14456.4
Fronious Symo 20.0-3-M 20 kW	6	2353.5	14121.0
ABB Trio-20.0-TL-OUTD 20 kW	6	2854.8	17128.8
SMA Sunny Tripower 20000 TL-30 20 kW	6	2229.8	13370.8
Danfoss FLX Pro 15 15 kW	8	1924.0	15392.0
SAMIL SolarLake 17000TL 17kW	7	1643.2	11502.4
Other costs		Price per Wp	Total Cost
Cables, transportation, labor, etc.		0.26	34060

Table 8.1 Prices of the chosen systems components

Table 8.2. shows the total investments for each whole system and the calculated simple payback times. The price of the produced energy in Estonia is chosen as 0.042 euro/kWh [23] and the subsidies paid for renewable energy is chosen as 0.0537 euro/kWh [24].

System	Total Investment (Euro)	Yearly Energy Production (kWh)	Simple Payback Time (Years)
Kostal PIKO 20 kW	145886.2	117500	12.9
KACO Powador 48.0 TL3 Park M 40kW	145641.4	118600	12.8
Fronious Symo 20.0-3-M 20 kW	145306.0	118200	12.8
ABB Trio-20.0-TL-OUTD 20 kW	148313.8	118600	13.0
SMA Sunny Tripower 20000 TL-30 20 kW	144563.8	118300	12.7
Danfoss FLX Pro 15 15 kW	146577.0	117700	12.9
SAMIL SolarLake 17000TL 17kW	142687.4	117500	12.6

Table 8.2 Calculated simple payback times for each system

9. Conclusions

Results of the simulations that are carried out to optimize the project shows that slightly better power production and performance ratios can be achieved by using different types of inverters for this project. Considering the initial investment prices, best economical results are achieved using seven SAMIL SolarLake 17000TL 17kW inverters. Performance ratios and normalized productions per months of this simulation are shown in Figure 9.1. and Figure 9.2. , respectively.

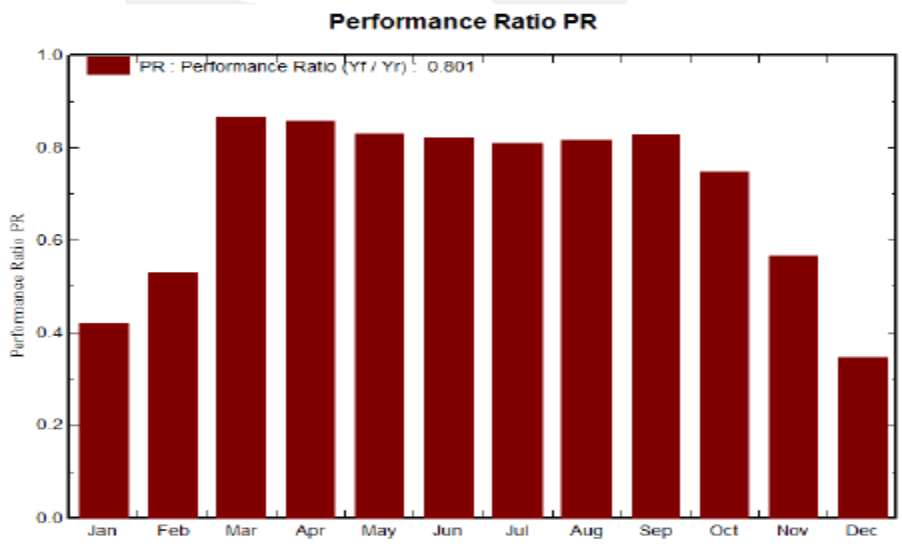

Figure 9.1. Performance ratios per month using SAMIL SolarLake 17000TL 17kW inverter

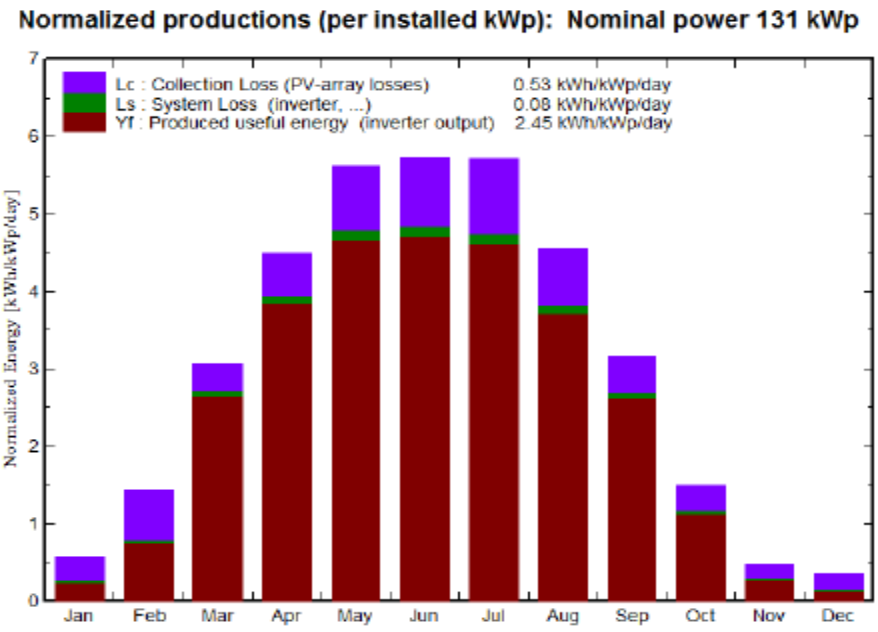

Figure 9.2. Normalized production per month using SAMIL SolarLake 17000TL 17kW inverter

Simulations that are carried out using SMA, KACO and ABB inverters have better output results but the initial costs of these systems are a bit higher. Considering the performance ratio and the power output of the system that uses SMA inverters, it can also be a valuable option. Performance ratios and normalized productions per months of this simulation are shown in Figure 9.3 and Figure 9.4 , respectively.

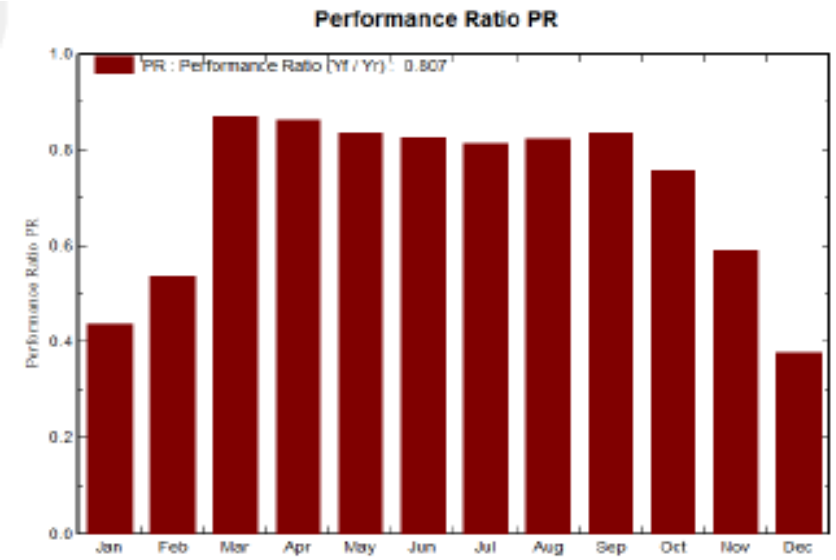

Figure 9.3 Performance ratios per month using SMA Sunny Tripower 20000 TL-30 20 kW

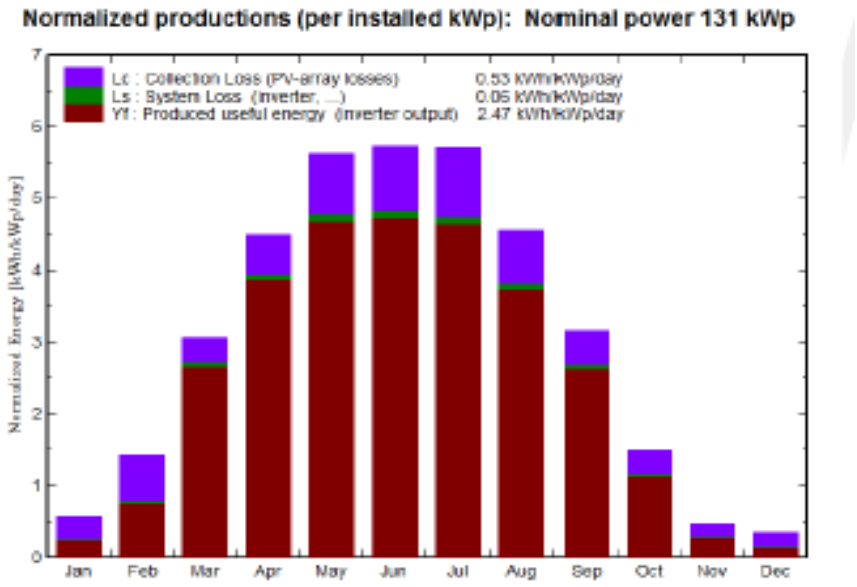

Figure 9.4 Normalized production per month using SMA Sunny Tripower 20000 TL-30 20kW

Current economical value of rooftop PV systems in Estonia are feasible considering the low simple payback times of 12 to 13 years and the lifetime of the project, which is considered 25 years.

10. Resume

A ground-mounted rooftop PV system for a shopping center in Tartu has been designed and optimized considering the technologies that are chosen by the company with the aim of producing the highest amount of energy possible using PVSyst software, which is widely used

in the industry. It has a large database of modules and inverters, 3D planning option, detailed presentations of simulation results. After running simulations for different tilt angles using two different inverters, it is seen that the best results are achieved using the tilt angle of 19° . Using this as a reference, different combinations of inverters have been chosen in order to investigate the change in power production and payback times.Simulations show that there are slight differences in power production and payback times between different systems using different inverters. Considering that both PV modules and inverter prices are expected to drop with the development in the technologies, more economically valuable results can be achieved in the future in Estonia.

11. Resümee

Käesolevas magistritöös on projekteeritud Tartu kaubanduskeskuse katusele päikepaneelide süsteem. Projekteerimisel on kasutatud simulatsiooniprgrammi PVSyst, mille abil on võimalik valida suurima tootlikkusega päikespaneelide süsteem ja inverter ning esitada 3D mõõtkavas simulatsiooni tulemused reaalses olukorras. Analüüsi tulemusena leiti, et päikesepaneelide optimaalne kaldenurk on 19 kraadi ja lähtuvalt sellest analüüsiti süteemi tootlikkust ja tasuvusaega erinevate inverteriga. Simulatsiooni tulemustest järeldati, et erinvate päikesepaneelide ja invereterite vahel ei ole suurt erinevust. Arvestades, et päikepaneelide ja toetavate süsteemide hinnad on langustrendis, on päikesepaneelide kasutamine Tartus antud näite alusel perspektiivne.

12. References

[1] European Comission. [Online] http://ec.europa.eu/energy/renewables/index_en.htm.

[2] *Estonia 2013 - Energy Policies Beyond IEA Countries.* International Energy Agency. p. 5.

[3] **FOSTER, Robert, GHASSEMI, Majid and COTA, Alma.** *Solar energy: renewable energy and the environment.* s.l. : CRC Press, 2009. pp. 4-7.

[4] **Kahle, A. B., et al.** RADIATION (SOLAR). *Proceedings of the IEEE.* 2003, 63, pp. 137-147.

[5] *Planning and Installing Photovoltaic Systems: A Guide for Installers, Architects and Engineers.* s.l. : Earthscan, 2003, DEUTSCHE GESELLSCHAFT FÜR SONNENENERGIE, pp. 8-10.

[6] http://meteonorm.com/images/uploads/demo_uploads/ghi_world_mn71.png.

[7] *Technology Fundamentals - The Sun as an Energy Resource.* **Quaschning, Volker.** 6, 2003, Renewable Energy World, pp. 90-93.

[8] **KALOGIROU, Soteris A.** *Solar energy engineering: processes and systems Academic Press.* s.l. : Academic Press, 2013. p. 469.

[9] **GTM Research/SEIA: U.S. Solar Market Insight.** *U.S.Solar Market Insight Report 2014 Q4.* 2014.

[10] *Global Market Outlook For Photovoltaics 2013-2017.* European Photovoltaic Industry Association. 2013. p. 4.

[11] *Market Report 2013.* European Photovoltaic Industry Association . 2013. pp. 2-3.

[12] **International Energy Agency.** *Snapshot of Global PV Markets.* 2014. pp. 4-12.

[13] **University of Geneva.** PVSyst Contextual Help. [Online] http://www.pvsyst.com.

[14] **Engel-Cox, J.A. et al.** Evaluation of Solar and Meteorological Data Relevant to Solar Energy Technology Performance in Malaysia. 2013, Vol. 3, 115-124.

[15] http://www.weatherbase.com/weather/weather.php3?s=24262&cityname=Tartu-Estonia.

[16] **Haberlin, Heinrich.** *Photovoltaics: System Design and Practice.* s.l. : John Wiley & Sons, Ltd., 2013. pp. 27-133.

[17] http://www.pvstudent.com/Inter-row-spacing-calculators.html.

[18] http://solarprofessional.com/articles/design-installation/q-a-calculating-inter-row-spacing.

[19] **International Electrotechnical Commission.** *Photovoltaic System Performance Monitoring - Guidelines for Measurement, Data Exchange and Analysis.* 1998. IEC 61274.

[20] *Uncertainty in Long-Term Photovoltaic Yield Predictions.* **Thevenard, Didier.** s.l. : Canmet Energy, 2010, p. 19.

[21] **Sustainable Energy Authority of Ireland.** Best Practice Guide For Photovoltaics. 2015, p. 67.

[22] **Washington State Department of Ecology.** *Ecology Information Document.* 2000. p. 1, Cost Analysis for Pollution Prevention.

[23] http://www.esro.ee/elekter/elektri-muuk/.

[24] http://elering.ee/renewable-energy-subsidy-2/.

[25] http://www.enfsolar.com/ApolloF/solar/Product/pdf/Crystalline/54f5421fed4d4.pdf.

[26] http://www.enfsolar.com/ApolloF/solar/Product/pdf/Inverter/54db1d9546f88.pdf.

[27] http://kaco-newenergy.com/fileadmin/data/downloads/products/TL3_Inverters_Powador_48.0_TL3_Park___.0_TL3_Park/Data%20Sheets/DTS_PW_48_72_TL3_en_150413.pdf.

[28] http://www.fronius.com/cps/rde/xbcr/SID-016A33A9-D825DA54/fronius_international/SE_DS_Fronius_Symo_EN_320473_snapshot.pdf.

[29]http://www09.abb.com/global/scot/scot232.nsf/veritydisplay/7d0fefe8e335cd0a85257e11006f0042/$file/TRIO-20.0-27.6-Rev-0.1.pdf.

[30] http://files.sma.de/dl/24336/STP25000TL-30-DEN1513-V20web.pdf.

[31] http://www.enfsolar.com/ApolloF/solar/Product/pdf/Inverter/53071676940eb.pdf.

APPENDIX 1

www.hhi-green.com/solar/en
www.facebook.com/hyundaisolar.eu

Hyundai Solar Module

Hyundai Heavy Industries was founded in 1972 and is a Fortune 500 company. The company employs more than 48,000 people, and has a global leading 7 business divisions with sales of 51.3 Billion USD in 2013. As one of our core businesses of the company, Hyundai Heavy Industries is committed to develop and invest heavily in the field of renewable energy.
Hyundai Solar is the largest and the longest standing PV cell and module manufacturer in South Korea. We have 600 MW of module production capacity and provide high-quality solar PV products to more than 3,000 customers worldwide. We strive to achieve one of the most efficient PV modules by establishing an R&D laboratory and investing more than 20 Million USD on innovative technologies.

RG-Series

Multi-crystalline Type
HiS-M250RG | HiS-M255RG | HiS-M260RG

Mono-crystalline Type
HiS-S260RG | HiS-S265RG | HiS-S270RG

Mechanical Characteristics

Dimensions	998 mm (39.29″)(W) × 1,640 mm (64.57″)(L) × 35 mm (1.38″)(H)
Weight	Approx. 17.2 kg (37.9 lbs)
Solar cells	60 cells in series (6 ×10 matrix) (Hyundai cell, Made in Korea)
Output cables	4 mm² (12AWG) cables with polarized weatherproof connectors, IEC certified (UL listed), Length 1.0 m (39.4″)
Junction box	IP68, weatherproof, IEC certified (UL listed)
Bypass diodes	3 bypass diodes to prevent power decrease by partial shade
Construction	Front : High transmission low-iron tempered glass, 2.8 mm (0.11″) Encapsulant : EVA Back Sheet : Weatherproof film
Frame	Clear anodized aluminum alloy type 6063 (silver or black color)

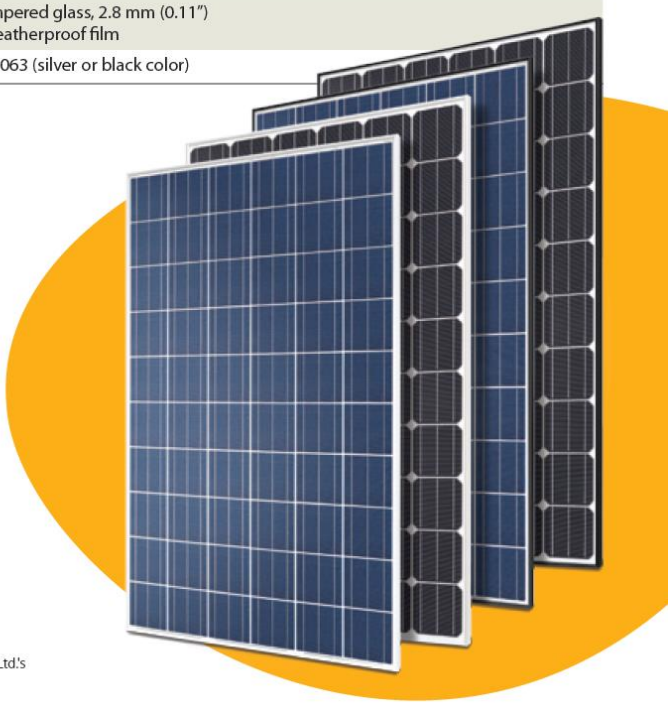

High Quality

- IEC 61215 (Ed.2) and IEC 61730 Certified by VDE
- UL listed (UL 1703), Class C Fire Rating
- Output power tolerance +3/-0 %
- ISO 9001:2008, ISO 14001:2004 and ISO 50001:2011 Certified
- OHSAS 18001:2007 Certified
- Advanced Mechanical Test (8,000 Pa) Passed (IEC 61215) / Mechanical Load Test (40 lbs/ft²) Passed (UL)
- IEC 62716 (Ammonia Corrosion Test) Certified
- IEC 61701 (Salt Mist Corrosion Test) Certified

Accredited Test Lab

- VDE (Test Data Acceptance Program)
- UL (Witness Test Data Program)

Limited Warranty

- 10 years for product defect
- 10 years for 90 % of warranted min. power
- 25 years for 80 % of warranted min. power

※ **Important Notice on Warranty**
The warranties apply only to the PV modules with Hyundai Heavy Industries Co., Ltd.'s logo (shown below) and product serial number on it.

HYUNDAI HEAVY INDUSTRIES

Electrical Characteristics

| Multi-crystalline Type |

		HiS-M□□□RG		
		250	255	260
Nominal output (Pmpp)	W	250	255	260
Voltage at Pmax (Vmpp)	V	30.9	31.0	31.1
Current at Pmax (Impp)	A	8.1	8.2	8.4
Open circuit voltage (Voc)	V	37.4	37.6	37.7
Short circuit current (Isc)	A	8.7	8.8	8.9
Output tolerance	%	+3/-0		
No. of cells & connections	pcs	60 in series		
Cell type	-	6" Multi-crystalline silicon (Hyundai cell, Made in Korea)		
Module efficiency	%	15.3	15.6	15.9
Temperature coefficient of Pmpp	%/K	-0.43	-0.43	-0.43
Temperature coefficient of Voc	%/K	-0.32	-0.32	-0.32
Temperature coefficient of Isc	%/K	0.048	0.048	0.048

※ All data at STC (Standard Test Conditions). Above data may be changed without prior notice.

| Mono-crystalline Type |

		HiS-S□□□RG		
		260	265	270
Nominal output (Pmpp)	W	260	265	270
Voltage at Pmax (Vmpp)	V	31.1	31.3	31.4
Current at Pmax (Impp)	A	8.4	8.5	8.6
Open circuit voltage (Voc)	V	37.9	38.1	38.2
Short circuit current (Isc)	A	8.9	9.0	9.2
Output tolerance	%	+3/-0		
No. of cells & connections	pcs	60 in series		
Cell type	-	6" Mono-crystalline silicon (Hyundai cell, Made in Korea)		
Module efficiency	%	15.9	16.2	16.5
Temperature coefficient of Pmpp	%/K	-0.45	-0.45	-0.45
Temperature coefficient of Voc	%/K	-0.33	-0.33	-0.33
Temperature coefficient of Isc	%/K	0.032	0.032	0.032

※ All data at STC (Standard Test Conditions). Above data may be changed without prior notice.

| Module Diagram |

(unit : mm, inch)

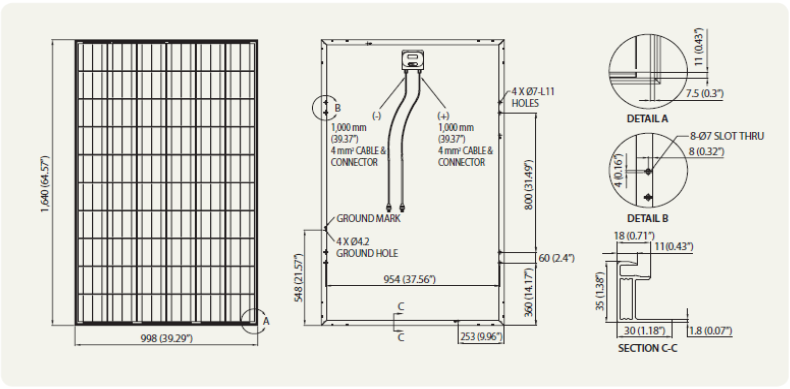

| I-V Curves |

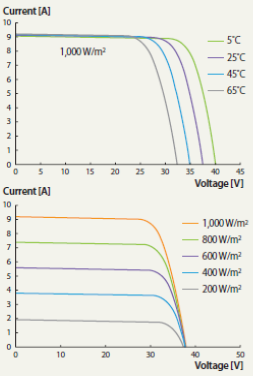

| Installation Safety Guide |

- Only qualified personnel should install or perform maintenance.
- Be aware of dangerous high DC voltage.
- Do not damage or scratch the rear surface of the module.
- Do not handle or install modules when they are wet.

Nominal Operating Cell Temperature	46°C ± 2
Operating Temperature	-40 - 85°C
Maximum System Voltage	DC 1,000 V (IEC) DC 600 V (UL)
Maximum Reverse Current	15 A

[Printed Date : February 2015]

Sales & Marketing
2nd Fl., Hyundai Bldg., 75, Yulgok-ro, Jongno-gu, Seoul 110-793, Korea
Tel : +82-2-746-8406, 7422, 8451 Fax : +82-2-746-7675

HYUNDAI HEAVY INDUSTRIES

Figure A1-1. Hyundai HIS-S250RG (25)

Technical data PIKO 20

- 3-phase feed-in
- Transformerless converting
- Integrated electronic DC switch
- Broad input voltage range
- Standard integrated communication package with data logger, web server, solar portal and the following interfaces: 2x Ethernet, RS485, S0, 4x analogue inputs (e.g. for ripple control receivers or PIKO Sensor)
- PIKO BA Sensor can be connected for the measurement of building consumption and for dynamic active power control
- Integrated switch contact for self-consumption optimisation
- Smart Home-ready, EEBus 1.0-ready

Input side (DC)

Max. PV power (cos φ = 1)	kWp	22.6
Rated input voltage ($U_{DC,r}$)	V	680
Max. input voltage (U_{DCmax})	V	1000
Min. input voltage (U_{DCmin})	V	160
Start-up input voltage ($U_{DCstart}$)	V	180
Max. MPP voltage (U_{MPPmax})	V	800
Min. MPP voltage for DC rated output in single tracker mode (U_{MPPmin})	V	–
Min. MPP voltage for DC rated output in two-tracker mode (U_{MPPmin})	V	515
Min. MPP voltage for DC rated output in three-tracker mode (U_{MPPmin})	V	345
Max. input current (I_{DCmax})	A	sym.: 20/20/20, unsym.: 20/20/20
Max. input current with parallel connection (input DC1+DC2/DC3)	A	40/20
Number of DC inputs		3
Number of independent MPP trackers		3

Output side (AC)

Rated output, cos φ = 1 ($P_{AC,r}$)	kW	20
Max. output apparent power, cos $\varphi_{,adj}$	kVA	20
Max. output voltage (U_{ACmax})	V	264.5
Min. output voltage (U_{ACmin})	V	184
Rated output current	A	29
Max. output current (I_{ACmax})	A	32.2
Short-circuit current (peak/RMS)	A	51/36.5
Grid connection		3/N/PE, AC, 400V
Rated frequency (f_r)	Hz	50
Max. grid frequency (f_{max})	Hz	51.5
Min. grid frequency (f_{min})	Hz	47.5
Setting range of the power factor cos $\varphi_{AC,r}$		0.80...1...0.80
Power factor for rated power (cos $\varphi_{AC,r}$)		1
Max. total harmonic distortion	%	3

Device properties

Max. total night-time consumption (own requirements standby)	W	2.15
Max. night-time consumption of communication board	W	2

Efficiency

Max. efficiency	%	98.0
European efficiency	%	97.3
MPP adjustment efficiency	%	99.9

Warranty

Warranty (years)		5
Warranty extension optional (years)		10/20

System data

Topology: Without galvanic separation - transformerless		✓
Internal protection according to IEC 60529		IP 55
Protective class according to IEC 62103		I
Overvoltage category according to IEC 60664-1 Input side (PV generator)		II
Overvoltage category according to IEC 60664-1 Output side (grid connection)		III
Degree of contamination		3
Environmental category (outdoor installation)		✓
Environmental category (interior installation)		✓
UV resistance		✓
Minimum cable cross-section of AC connecting line	mm^2	6
Minimum cable cross-section of DC connecting line	mm^2	4
Max. fusing on output side		B40, C40
Operator protection (EN 62109-2)		RCCB Typ B
Electronic disconnection device integrated		✓
Height	mm	540 (21.26 in)
Width	mm	700 (27.56 in)
Depth	mm	265 (10.43 in)
Weight	kg	48.5 (106.9 lb)
Cooling principle - convection		–
Cooling principle - regulated fans		✓
Max. air throughput	m^3/h	2x84
Max. noise emission	dBA	56
Ambient temperature	°C	-20...60 (-4...140 °F)
Max. installation altitude above sea level	m	2000 (6562 ft)
Relative humidity	%	4...100
Connection technology at input side - MC 4		✓
Connection technology at output side - spring-loaded terminal strip		✓

Interfaces

Ethernet RJ45		2
RS485		1
S0		1
Analogue inputs		4
PIKO BA Sensor Interface		1

Efficiency characteristics of PIKO 20

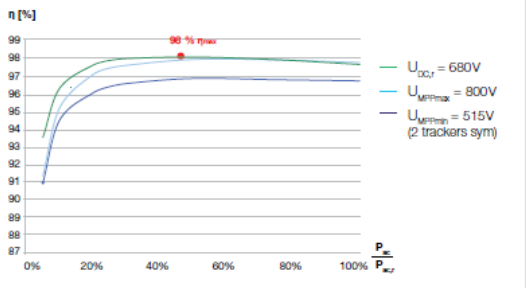

Smart connections.

Contact

KOSTAL Solar Electric GmbH
Hanferstr. 6
79108 Freiburg i. Br.
Germany

Tel. +49 761 477 44 - 100
Fax +49 761 477 44 - 111

www.kostal-solar-electric.com

Figure A1-2. Kostal PIKO 20 kW (26)

Technical data

Powador 48.0 TL3 Park | 72.0 TL3 Park

Electrical data	48.0 TL3 Park	72.0 TL3 Park
Input variables		
MPP range	200 V ... 800 V*	200 V ... 850 V**
Starting voltage	250 V	250 V
No-load voltage	1000 V	1000 V
Max. input current	3x34.0 A	3x36.0 A
Number of MPP trackers	3	3
Max. power/tracker	20 kW	24 kW
Number of strings	3x1 based on design M 3x4 based on design XL	3x1 based on design M 3x5 based on design XL 3x4 based on design XL-F
Output variables		
Rated output (@ 277 V)	40000 VA	60000 VA
Line voltage	480 V / 277 V (3 / N / PE)	480 V / 277 V (3 / N / PE)
Rated current	3x48.1 A	3x72.2 A
Rated frequency	50 Hz / 60 Hz	50 Hz / 60 Hz
cos phi	0.80 inductive ... 0.80 capacitive	0.80 inductive ... 0.80 capacitive
Number of grid phases	3	3
General electrical data		
Max. efficiency	98.0 %	98.3 %
European efficiency	97.9 %	98.0 %
Night consumption	1.5 W	1.5 W
Switching plan	transformerless	transformerless
Certifications	overview: see homepage / download area	overview: see homepage / download area
Mechanical data		
Display	graphical display + LEDs	graphical display + LEDs
Control units	4-way navigation + 2 buttons	4-way navigation + 2 buttons
Interfaces	Ethernet, USB, RS485, S0 output, digital input "inverter off"	Ethernet, USB, RS485, S0 output, digital input "inverter off"
Fault signalling relay	potential-free NOC max. 230 V / 1 A	potential-free NOC max. 230 V / 1 A
Connections	AC connection via screw terminals, bushing, 1 x M50, max cross section: 50 mm² (flexible); DC connection of M version: spring-type terminals 6-35 mm² ***; DC connection of XL version: screw and spring-type terminals 10 mm², bushing 48.0 TL3 Park 6 x M32 / 72.0 TL3 Park 6 x M40	
Ambient temperature	-20 °C ... +60 °C****	-20 °C ... +60 °C****
Cooling	fan, max. 600 m³ / h	fan, max. 600 m³ / h
Protection class	IP54	IP54
Noise emission	58 dB (A) (only fan noise)	58 dB (A) (only fan noise)
DC switch	integrated	integrated
H x W x D	1360 x 840 x 355 mm	1360 x 840 x 355 mm
Weight	151 kg	173 kg
Product variants		
Version M	DC switch	
Version XL	DC switch / fuse protection DC input plus / overvoltage protection type 2	
Version XL-SPD 1+2	DC switch / fuse protection DC input plus / overvoltage protection type 1 + 2	
Version XL-F	DC switch / fuse protection DC input plus and minus / overvoltage protection type 2	
Version XL-F-SPD1+2	DC switch / fuse protection DC input plus and minus / overvoltage protection type 1 + 2	

* The possible input power is reduced at voltages lower than 410 V. The input current is limited to 34.0 A per input. ** The possible input power is reduced at voltages lower than 580 V. The input current is limited to 36.0 A per input. *** Only in conjunction with external Powador Mini-Argus **** Power derating at high ambient temperatures Conforms to the country-specific standards and regulations according to the country version that has been set.

Figure A1-3. KACO Powador 48.0 TL3 Park M 40kW (27)

TECHNICAL DATA FRONIUS SYMO (10.0-3-M, 12.5-3-M, 15.0-3-M, 17.5-3-M, 20.0-3-M)

INPUT DATA	SYMO 10.0-3-M	SYMO 12.5-3-M	SYMO 15.0-3-M	SYMO 17.5-3-M	SYMO 20.0-3-M
Max. input current ($I_{dc\ max\ 1}$ / $I_{dc\ max\ 2}$)	27.0 A / 16.5 A		33.0 A / 27.0 A		
Max. array short circuit current (MPP_1/MPP_2)	40.5 A / 24.8 A		49.5 A / 40.5 A		
Min. input voltage ($U_{dc\ min}$)	200 V				
Feed-in start voltage ($U_{dc\ start}$)	200 V				
Nominal input voltage ($U_{dc,r}$)	600 V				
Max. input voltage ($U_{dc\ max}$)	1,000 V				
MPP voltage range ($U_{mpp\ min}$ – $U_{mpp\ max}$)	270 - 800 V	320 - 800 V		370 - 800 V	420 - 800 V
Number MPP trackers	2				
Number of DC connections	3+3				

OUTPUT DATA	SYMO 10.0-3-M	SYMO 12.5-3-M	SYMO 15.0-3-M	SYMO 17.5-3-M	SYMO 20.0-3-M
AC nominal output ($P_{ac,r}$)	10,000 W	12,500 W	15,000 W	17,500 W	20,000 W
Max. output power	10,000 VA	12,500 VA	15,000 VA	17,500 VA	20,000 VA
Max. output current ($I_{ac\ max}$)	16.0 A	19.9 A	23.9 A	27.9 A	31.9 A
Grid connection (voltage range)	3-NPE 400 V / 230 V or 3-NPE 380 V / 220 V (+20 % / -30 %)				
Frequency (Frequency range)	50 Hz / 60 Hz (45 - 65 Hz)				
Total harmonic distortion	< 2 %				
Power factor ($\cos \varphi_{ac,r}$)	0 - 1 ind. / cap.				

GENERAL DATA	SYMO 10.0-3-M	SYMO 12.5-3-M	SYMO 15.0-3-M	SYMO 17.5-3-M	SYMO 20.0-3-M
Dimensions (height x width x depth)	725 x 510 x 225 mm				
Weight	34.8 kg		43.4 kg		
Degree of protection	IP 66				
Protection class	1				
Overvoltage category (DC / AC) [1]	2 / 3				
Night time consumption	< 1 W				
Inverter design	Transformerless				
Cooling	Regulated air cooling				
Installation	Indoor and outdoor installation				
Ambient temperature range	-25 - +60 °C				
Permitted humidity	0 - 100 %				
Max. altitude	2,000 m / 3,400 m (unrestricted / restricted voltage range)				
DC connection technology	6x DC+ and 6x DC- screw terminals 2.5 - 16 mm^2				
Mains connection technology	5-pole AC screw terminals 2.5 - 16 mm^2				
Certificates and compliance with standards	ÖVE / ÖNORM E 8001-4-712, DIN V VDE 0126-1-1/A1, VDE AR N 4105, IEC 62109-1/-2, IEC 62116, IEC 61727, AS 3100, AS 4777-2, AS 4777-3, CER 06-190, G83/2, G59/3, UNE 206007-1, SI 4777, CEI 0-16, CEI 0-21				

[1] According to IEC 62109-1. DIN rail for optional overvoltage protection (type 2) is included.
Further information regarding the availability of the inverters in your country can be found at www.fronius.com.

Figure A1-4. Fronious International Symo 20.0-3-M 20 kW (28)

Technical data and types

Type code	TRIO-20.0-TL-OUTD	TRIO-27.6-TL-OUTD
Nominal output power	20000W	27600W
Maximum output power	22000W[1]	30000W[1]
Rated grid AC voltage	480V	
Input side (DC)		
Number of independent MPPT channels	2; Programmable for 1 MPPT	
Maximum usable power for each MPPT channel	12000W	16000W
Absolute maximum voltage (V_{max})	1000V	
Start-up voltage (V_{start})	360V (adj. 250-500V)	
Full power MPPT voltage range	450-800V	520-800V
Operating MPPT voltage range	200-950V	
Maximum usable current (Idc max) per MPPT channel	25.0A	30.9A
Maximum short circuit current (Isc max) per MPPT channel	30.0A	36.0A
Number of inputs (strings) per MPPT channel	-S version: 1; -S1, -S1A, -S1B versions: 4	
Array wiring termination type	Terminal block, screw terminal, copper only, -S: 12AWG-2AWG; -S1, -S1A, -S1B: 12AWG-6AWG	
Output side (AC)		
Grid connection type	3Ø/4W + Ground	
Default operating voltage range	422-528V	
Extended adjustable voltage range	240-552V[2]	
Nominal grid frequency	60Hz	
Adjustable grid frequency range	57-63Hz	
Continuous current	27.0 A_{RMS}	36.0 A_{RMS}
Contributory fault current (@ 1 cycle)	51.4A_{RMS}	42.72A_{RMS}
Power factor	> 0.995 (adj. ±0.8, or ±0.9 for active power >20kW)	>0.995 (adj. ± 0.8, or ±0.9 for active power >27.6kW)
Total harmonic distortion at rated power	<3%	
Grid wiring termination type	Pass-through terminal. Tension clamp. Copper 8AWG-4AWG	Pass-through terminal. Tension clamp. Copper 6AWG-4AWG
Input protection devices		
Reverse polarity protection	Yes, passive inverter protection only.[3]	
Supplementary over-voltage protection type for each MPPT	-S1, -S1A, -S1B version: plug-in class II modular surge arrestor	
PV array ground fault detection	Meets UL1741/NEC requirements	
Output protection devices		
Anti-islanding protection	Meets UL 1741 / IEEE 1547 requirements	
Supplementary over-voltage protection type	-S1A version: plug-in class II modular surge arrestor	
Optional AC fused disconnect current rating (per contact)	-S1B version: 35A	-S1B version: 45A
Maximum AC OCPD rating	40A	50A
Operating performance		
Efficiency (Max/CEC)	98.2% / 97.5%	
Feed-in power threshold	65W_{RMS}	70W_{RMS}
Communication		
User-interface display	5.5" x 1.25" graphic display	
Standard communication interfaces	(1) RS485 connection, can be configured for Aurora protocol or Modbus RTU. Support for optional monitoring expansion cards.	
Optional remote monitoring logger	VSN 700	
Environmental		
Ambient operating temperature range	-22°F to +140°F (-30°C to +60°C) Derating above +113°F (45°C)	
Ambient storage temperature range	-40°F to +185°F (-40°C to +85°C)	
Relative humidity	0-100% condensing	
Acoustic noise emission level	<50 db (A) @1m	
Maximum operating altitude without derating	6560ft (2000m)	
Mechanical specifications		
Enclosure rating	NEMA 4X	
Cooling	Natural convection	
Dimensions H x W x D	41.7 x 27.6 x 11.5 in. / 1061 x 702 x 292 mm.	
Unit weight	157lb (71kg)	168lb (76kg)
Conduit connections	Bottom: (2) concentric DC KOs 1", 1 1/2" on removable plate, (2) 1/2" plugged comm. openings, (1) 1" plugged AC opening	
Mounting system	Wall bracket	

1. Capability enabled within maximum input current, maximum input power, maximum output current, ambient operating temperature limits, and power factor at unity.
2. Extended voltage range is for trip settings only, not operational voltage ranges.
3. In -S1, -S1A and -S1B models, the string polarity must be verified before connection. Please refer to installation manual for the correct installation procedure.

Figure A1-5. ABB Trio-20.0-TL-OUTD 20 kW (29)

Technical Data	Sunny Tripower 20000TL	Sunny Tripower 25000TL
Input (DC)		
Max. DC power (@ cos φ = 1) / DC rated power	20440 W / 20440 W	25550 W / 25550 W
Max. input voltage	1000 V	1000 V
MPP voltage range / rated input voltage	320 V to 800 V / 600 V	390 V to 800 V / 600 V
Min. input voltage / start input voltage	150 V / 188 V	150 V / 188 V
Max. input current input A / input B	33 A / 33 A	33 A / 33 A
Number of independent MPP inputs / strings per MPP input	2 / A:3; B:3	2 / A:3; B:3
Output (AC)		
Rated power (@ 230 V, 50 Hz)	20000 W	25000 W
Max. AC apparent power	20000 VA	25000 VA
AC nominal voltage	3 / N / PE; 220 / 380 V 3 / N / PE; 230 / 400 V 3 / N / PE; 240 / 415 V	
AC voltage range	180 V – 280 V	
AC grid frequency / range	50 Hz / 44 Hz ... 55 Hz 60 Hz / 54 Hz ... 65 Hz	
Rated power frequency / rated grid voltage	50 Hz / 230 V	
Max. output current / Rated output current	29 A / 29 A	36,2 A / 36,2 A
Power factor at rated power / Adjustable displacement power factor	1 / 0 overexcited to 0 underexcited	
THD	≤ 3 %	
Feed-in phases / connection phases	3 / 3	
Efficiency		
Max. efficiency / European Efficiency	98.4 % / 98.0 %	98.3 % / 98.1 %
Protective devices		
DC-side disconnection device	●	
Ground fault monitoring / grid monitoring	● / ●	
DC surge arrester (Type II) can be integrated	o	
DC reverse polarity protection / AC short-circuit current capability / galvanically isolated	● / ● / –	
All-pole sensitive residual-current monitoring unit	●	
Protection class (according to IEC 62109-1) / overvoltage category (according to IEC 62109-1)	I / AC: III; DC: II	
General data		
Dimensions (W / H / D)	661 / 682 / 264 mm (26.0 / 26.9 / 10.4 inch)	
Weight	61 kg (134.48 lb)	
Operating temperature range	-25 °C to +60 °C (-13 °F to +140 °F)	
Noise emission (typical)	51 dB(A)	
Self-consumption (at night)	1 W	
Topology / cooling concept	Transformerless / Opticool	
Degree of protection (as per IEC 60529)	IP65	
Climatic category (according to IEC 60721-3-4)	4K4H	
Maximum permissible value for relative humidity (non-condensing)	100 %	
Features / function		
DC connection / AC connection	SUNCLIX / spring-cage terminal	
Display	-	
Interface: RS485, Speedwire/Webconnect	o / ●	
Data interface: SMA Modbus / SunSpec Modbus	● / ●	
Multifunction relay / Power Control Module	o / o	
OptiTrack Global Peak / Integrated Plant Control / Q on Demand 24/7	● / ● / ●	
Off-Grid capable / SMA Fuel Save Controller compatible	● / ●	
Guarantee: 5 / 10 / 15 / 20 / 25 years	● / o / o / o / o	
Certificates and permits (more available on request) * Does not apply to all national appendices of EN 50438	ANRE 30, AS 4777, BDEW 2008, C10/11:2012, CE, CEI 0-16, CEI 0-21, EN 50438*, G59/3, IEC 60068-2-x, IEC 61727, IEC 62109-1/2, IEC 62116, MEA 2013, NBR 16149, NEN EN 50438, NRS 097-2-1, PEA 2013, PPC, RD 1699/413, RD 661/2007, Res. n°7:2013, SI4777, UTE C15-712-1, VDE 0126-1-1, VDE-AR-N 4105, VFR 2014	
Type designation	STP 20000TL-30	STP 25000TL-30

Figure A1-6. • SMA Sunny Tripower 20000 TL-30 20 kW (30)

FLX Factsheet

For additional technical data and functional descriptions please refer to the design guide on www.danfoss.com/solar

Parameter	FLX Series								
AC									
Rated apparent power [1]	5 kVA	6 kVA	7 kVA	8 kVA	9 kVA	10 kVA	12.5 kVA	15 kVA	17 kVA
Rated active power [2]	5 kW	6 kW	7 kW	8 kW	9 kW	10 kW	12.5 kW	15 kW	17 kW
Reactive power range [1]	0-3.0 kVAr	0-3.6 kVAr	0-4.2 kVAr	0-4.8 kVAr	0-5.4 kVAr	0-6.0 kVAr	0-7.5 kVAr	0-9.0 kVAr	0-10.2 kVAr
Rated grid voltage (voltage range)	3P+N+PE – 230/400 V (+/- 20 %)								
Rated current AC	3x7.2 A	3x8.7 A	3x10.1 A	3x11.6 A	3x13.0 A	3x14.5 A	3x18.1 A	3x21.7 A	3x24.7 A
Max. current AC	3x7.5 A	3x9.0 A	3x10.6 A	3x12.1 A	3x13.6 A	3x15.1 A	3x18.8 A	3x22.6 A	3x25.6 A
AC current distortion (THD %)	–	–	–	–	–	–	<2%	<2%	<2%
Power factor – default	>0.99 at rated power								
Power factor – regulated	0.8 over-excited, 0.8 under-excited								
Standby consumption	2.7 W								
Rated grid frequency (frequency range)	50 Hz (+/- 5 Hz)								
DC									
Max. PV input power per MPPT	5.2 kW	6.2 kW	7.2 kW	8 kW					
Rated PV input power, total	5.2 kW	6.2 kW	7.2 kW	8.3 kW	9.3kW	10.4 kW	12.9 kW	15.5 kW	17.6 kW
Rated voltage DC	715 V								
MPP voltage range: Active tracking [3] / rated power [4]	220/250-800 V	220/260-800 V	220/300-800 V	220/345-800 V	220/390-800 V	220/430-800 V	220/360-800 V	220/430-800 V	220/485-800 V
Max. voltage DC	1000 V								
Start up voltage	250 V								
Turn off voltage	220 V								
Max. MPPT current DC	12.0 A per input								
Max. short circuit current DC	13.5 A per input								
MPP trackers/DC inputs	2 / 2 (Sunclix)						3 / 3 (Sunclix)		
Efficiency									
Max. Efficiency	–	97.8 %	–	97.9 %	–	98.0 %	98.0 %	98.0 %	98.0 %
EU efficiency at rated voltage DC	–	96.5 %	–	97.0 %	–	97.0 %	97.3 %	97.4 %	97.4 %
MPPT efficiency, static	99.9 %								
Enclosure									
Dimensions (H, W, D)/ incl. packaging	667x500x233 mm / 774x570x356 mm								
Weight	38 kg						39 kg		
Enclosure rating	IP 65								
Acoustic noise level [5]	–						55 db(A)		
Operational temperature range	-25 to +60 °C (Possible power derating above +45 °C)								
Relative humidity	95 % (non-condensing)								
Ancillary Services									
Active power	Fixed limit, set point curves, remotely controlled								
Reactive power	Constant, set point curves, remotely controlled								
Interfaces	Ethernet, RS 485								
Options	GSM Modem, sensor interface, PLA [6]								
Cooling concept	Fan								
Safety									
Approvals and certificates	See www.danfoss.com/solar -> downloads								
Electrical Safety	IEC 62109-1/IEC 62109-2 (Class I, grounded – communication part Class II, PELV)								
Functional Safety	Islanding detection/ loss of mains – tree-phase monitoring, active frequency shift and RoCoF, Voltage and frequency surveillance, DC content of AC current surveillance, Insulation resistance surveillance, RCMU – Type B								

1) At rated grid voltage.
2) At rated grid voltage, cosphi = 1.
3) To utilize the full range, asymmetrical layouts must be considered including start up voltage for at least one string. Achieving Nominal power will depend on configuration.
4) At symmetric input configuration.
5) SPL (Sound Pressure Level) at 1 m under normal operation conditions measured at 25°C.
6) For connecting e.g. radio ripple control receiver.

Danfoss Solar Inverters A/S | Nordborgvej 81 | DK-6430 Nordborg • Denmark
Tel: +45 7488 1300 | Fax: +45 7488 1301 | E-mail: solar-inverters@danfoss.com | www.danfoss.com/solar

Figure A1-7. • Danfoss FLX Pro 15 15 kW (31)